

Synthesis of the OECD/NEA-PSI CFD benchmark exercise

Michele Andreani*, Arnoldo Badillo, Ralf Kapulla

Paul Scherrer Institut (PSI), Laboratory for Thermal-Hydraulics, 5232 Villigen, Switzerland



HIGHLIGHTS

- A benchmark exercise on stratification erosion in containment was conducted using a test in the PANDA facility.
- Blind calculations were provided by nineteen participants.
- Results were compared with experimental data.
- A ranking was made.
- A large spread of results was observed, with very few simulations providing accurate results for the most important variables, though not for velocities.

ARTICLE INFO

Article history:

Received 30 November 2015

Accepted 7 December 2015

Available online 28 February 2016

ABSTRACT

The third International Benchmark Exercise (IBE-3) conducted under the auspices of OECD/NEA is based on the comparison of blind CFD simulations with experimental data addressing the erosion of a stratified layer by an off-axis buoyant jet in a large vessel. The numerical benchmark exercise is based on a dedicated experiment in the PANDA facility conducted at the Paul Scherrer Institut (PSI) in Switzerland, using only one vessel. The use of non-prototypical fluids (i.e. helium as simulant for hydrogen, and air as simulant for steam), and the consequent absence of the complex physical effects produced by steam condensation enhanced the suitability of the data for CFD validation purposes. The test started with a helium–air layer at the top of the vessel and air in the lower part. The helium-rich layer was gradually eroded by a low-momentum air/helium jet emerging at a lower elevation. Blind calculation results were submitted by nineteen participants, and the calculation results have been compared with the PANDA data. This report, adopting the format of the reports for the two previous exercises, includes a ranking of the contributions, where the largest weight is given to the time progression of the erosion of the helium-rich layer. In accordance with the limited scope of the benchmark exercise, this report is more a collection of comparisons between calculated results and data than a synthesis. Therefore, the few conclusions are based on the mere observation of the agreement of the various submissions with the test result, and do not entail any interpretation of the discrepancies, which is left to the individual participants.

© 2016 Elsevier B.V. All rights reserved.

1. Introduction

1.1. Background of the 3rd CFD benchmark exercise

Hydrogen generated during a (postulated) severe accident with core degradation is a major safety issue, because flammable hydrogen/air mixtures could form in the NPP containment, with a resulting risk of deflagration or detonation, which might challenge its structural integrity. The presence of hydrogen stratification is a special source of concern, as pockets of the gas mixture with a high

H_2 concentration could result in local dangerous conditions. A special concern is thus the build-up and persistence of stratification of hydrogen in certain regions. Various experimental programmes (Allelein et al., 2007; Deri et al., 2010; OECD/NEA THAI Project, 2010; Studer et al., 2012; Kapulla et al., 2013; Paladino et al., 2013) and code validation activities (Schwarz et al., 2011; Andreani et al., 2012; Kelm et al., 2014;) have included in-depth investigations on stratification formation and break-up/erosion processes. In the PIRT prepared by the WGAMA Special CFD Group (Smith, 2009), mixing and combustion phenomena in containment has been classified as one of the high-ranking issues for nuclear power plant safety, and one requiring CFD analysis. In order to promote the validation of CFD codes for the high-ranking safety issues, the Special CFD Group took the initiative to organise International Benchmark

* Corresponding author. Tel.: +41 56 310 2687; fax: +41 56 310 4481.

E-mail address: Michele.andreani@psi.ch (M. Andreani).

Nomenclature

CFD	computational fluid dynamics
CSNI	committee on the safety of nuclear installations
D_{AB}	molecular diffusivity (m^2/s)
FOV	field of view
IAEA	International Atomic Energy Authority
ILES	intrinsic large eddy simulation (LES)
LES	large eddy simulation (turbulence model)
MS	mass spectrometer
NEA	Nuclear Energy Agency
NPP	Nuclear Power Plant
OECD	Organisation for Economic Co-operation and Development
PIRT	phenomenon identification and ranking table
PIV	particle image velocimetry
RMS	root mean square
RSM	Reynolds stress model (turbulence model)
SAS	scale-adaptive simulation (turbulence model)
Sc_t	turbulent Schmidt number
SST	shear stress transport (turbulence model)
TC	thermocouple
TKE	turbulent kinetic energy (m^2/s^2)
Tu	turbulence intensity (%)
WGAMA	Working Group on the Analysis and Management of Accidents
ZLES/WALE	zonal large eddy simulation/wall adapting local eddy viscosity (turbulence model)

produced. The following information has been provided to potential participants to the benchmark: technical specifications, which include the details of the benchmark exercise; CAD drawings of the PANDA facility; results from off-line characterization tests on the velocity profiles at the outlet of the air–helium injection pipe; list of variables for which the participants were asked to submit their simulation results (X - Y files).

Blind calculation results, as well as essential information on the codes and models used for the simulations, were submitted by nineteen (19) participants. In consideration of the limited scope of the OECD/NEA CFD benchmark exercises (which cannot be compared with the CSNI International Standard Problems, ISP's) (e.g. Lübbesmeyer and Aksan, 2003; Allelein et al., 2007), no accompanying report was requested (OECD-NEA-PSI CFD, 2013), and thus no information could be gathered on mesh, modelling details, application of Best Practice Guidelines, etc. Therefore, due to the limited information available and the agreement that a first synthesis of the results would be prepared by the PSI team without any feed-back from the IBE-3 participants (similarly to the previous two exercises), this report does not include any analysis of the results, which is expected to be conducted by the individual participants. This report only includes the comparisons of the submitted variables with the corresponding experimental data, highlighting the agreement between calculations and results, and some observations on specific aspects of the simulations that deserve some analysis. In the following chapters, the word “synthesis” will still be used, but the reader is warned that this report is more a summary of the simulation activity than an actual wrap-up of the exercise. Nevertheless, the report will include some conclusions and suggestions that could be useful for the further analysis of the data, interpretation of the results and critical evaluation of models and their implementation in the codes.

This synthesis report, adopting the format of the reports for the two previous exercises, includes a ranking of the contributions, where the largest weight is given to the time progression of the erosion of the helium-rich layer. Due to the length of the experiment (7200 s), a few organisations could not complete the simulation of the entire transient before the submission deadline. The incomplete submissions have been accepted, but a system of penalties has been built in the ranking for fairly comparing all contributions.

1.3. Contents of the report

In consideration of the scope of the synthesis and the availability of a detailed description of the experiment used for the IBE-3 (Kapulla et al., 2014a), this synthesis includes only a brief description of the experiment and the few data that are used for the comparison with the submissions. For the complete presentation of the experimental results, the participants in the exercise are referred to (Kapulla et al., 2014b). The paper thus consists of:

- (1) brief description of the experiment and calculated variables to compare with experimental data;
- (2) summary of the submissions;
- (3) presentation of the main results for all submissions;
- (4) ranking of the contributions;
- (5) more detailed comparisons for the highest-ranked submissions and
- (6) conclusions (based on mere observations).

2. The experiment

2.1. Geometrical configuration

The PANDA facility is a multi-compartment, large-scale thermal-hydraulics test rig located at the Paul Scherrer Institute (PSI), Switzerland. Specifically for this CFD benchmark experiment

Exercises (IBE). The first two were related to primary system issues (Mahaffy, 2010; Smith et al., 2011, 2013; Lee et al., 2012). For the third exercise the topic of gas mixing in a containment in presence of hydrogen and initially stratified conditions was selected.

The third International Benchmark Exercise (IBE-3) conducted under the auspices of OECD/NEA is thus based on the comparison of blind CFD simulations with experimental data addressing the erosion of a stratified layer by a buoyant jet in a large vessel. The main objective of the activity is to evaluate the use of CFD for simulating flow mixing in a model containment volume for conditions of practical interest to nuclear reactor safety (Kapulla et al., 2014a).

Such is the case of the erosion of a stable hydrogen layer in a containment volume formed during a severe accident caused by the flow induced by buoyant jets. The numerical benchmark exercise is based on a dedicated experiment in the PANDA facility conducted at the Paul Scherrer Institut (PSI) in Switzerland (Kapulla et al., 2014a, 2014b). The use of non-prototypical fluids (i.e. helium as simulant for hydrogen, and air as simulant for steam), and the consequent absence of the complex physical effects produced by steam condensation enhanced the suitability of the data for CFD validation purposes. The new PANDA test was designed to investigate the gradual erosion of a helium–air layer at the top of a free volume caused by a low-momentum air/helium jet emerging at a lower elevation. It was thus intended to address the possibility of the permanence of hydrogen stratification just beneath the containment dome under conditions determined by a low velocity plume, which becomes negatively buoyant as it interacts with the density interface between the ambient fluid and the helium-rich layer above.

1.2. Format of the benchmark exercise

The PANDA experiment for the 3rd CFD benchmark exercise was completed, and the unique set of high-quality experimental data, including velocity measurements in the area of the interaction of the buoyant jet with the density interface, has been successfully

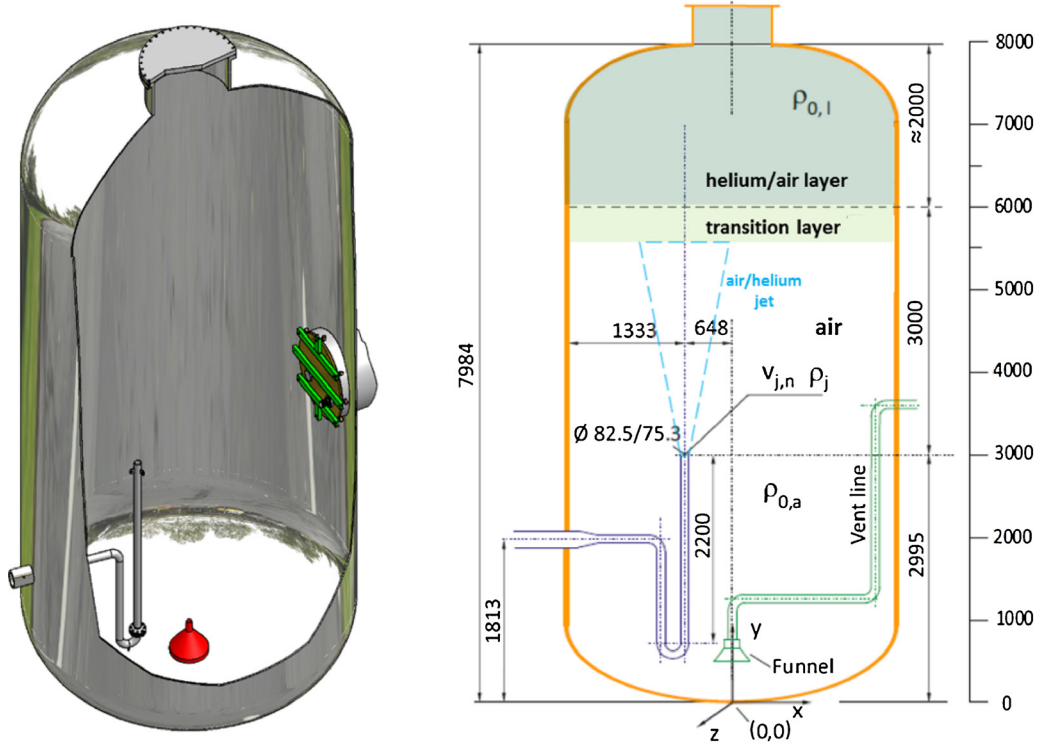


Fig. 1. Geometrical configuration for the experiment.

one compartment has been isolated from the other ones, and this vessel constitutes the test section (Fig. 1). The test vessel, 8 m in height, is composed of four sections, each of 4 m outer diameter but with varying inner diameters, depending on the local wall thickness. Two cylindrical sections make up the central part, with curved top and bottom caps welded on.

At the top of the test vessel a 980 mm diameter manhole exists (used for access purposes); its presence adds an extra 464 mm to the vessel internal height. All the sections are made from stainless steel (DIN 1.4571). The total enclosed volume within the vessel (including the manhole space) is 90.24 m³, and the total internal surface area (including the top and side manhole surfaces) is 108.49 m². A vertical injection line with internal diameter 75.3 mm and wall thickness 3.6 mm is placed at a horizontal distance of 647.5 mm (nominally 650 mm) from the axis of the test vessel. The outlet from the injection line is located 2995 mm (nominally 3000 mm) above the lowest point on the axis of the vessel and is positioned vertically to produce a jet directed upwards. The straight section of the inlet pipe upstream from the outlet orifice is more than 30 diameters in length. The pipe has been constructed specifically for this PANDA benchmark test. In order to keep the pressure constant, the air/helium mixture is vented to the atmosphere via a funnel oriented downwards (red component in Fig. 1) located just above (maximum gap ~160 mm) the base of the vessel. For convenience, the venting is made via the large interconnecting pipe (IP in Fig. 1), which has been blocked off specifically for this test. Note that the end of the interconnecting pipe is not flush with the inner surface of the PANDA vessel, but protrudes into it a distance of 190 mm. Details of the geometry (including technical drawings and CAD files) have been included in the technical documentation distributed to the benchmark participants.

2.2. Initial and boundary conditions

The experiment addressed the mixing produced by a vertical jet in a vessel where stratified conditions existed before the start

of the gas injection. A helium-lean mixture of air and helium was thus injected into the vessel, where initially a helium-rich layer occupied the upper region and pure air filled the volume below (Fig. 1). The experiment was conducted under ambient conditions: i.e. at nominal atmospheric pressure, measured internally in the vessel at 0.994 bar (standard deviation 0.003 bar). The gases in the vessel are nominally at room temperature and the temperature of the injected air/helium mixture is slightly elevated.

The PANDA vessel and the major internal penetrations/flanges are made of stainless steel. All external surfaces are insulated. The heat losses from all the PANDA vessels have been experimentally determined over a range of temperatures much higher than those encountered in the present test. The present test is carried out at ambient temperature (nominally 20 °C), except for the slightly elevated temperature of the incoming air/helium mixture at the injection pipe outlet. Consequently, the heat losses in this test are considered to be small over its duration (2 h).

Prior to the test, stratified air/helium conditions have been created in the test vessel. A helium-rich layer occupies the region $h > 5000$ mm (measured from the lowest point on the inside of the vessel, this being 11,700 mm above the concrete base mat of the PANDA building), while air fills the region below this layer. The measured helium and air molar fractions at time $t = 0$ as a function of elevation are displayed in Fig. 2. This Figure is compiled from mass spectroscopy measurements taken principally along the axis of the vessel. However, a number of off-axis measurements have also been included to demonstrate the horizontal homogeneity of the gas mixture composition. The molar fraction of helium was zero for $h < 5000$ mm, and increased non linearly with height to around 0.37 helium molar fraction at elevation $h = 8000$ mm (the virtual height of the vessel in the absence of the manhole), and above into the manhole space itself. The water vapour concentrations were between 0.7 and 1.5%, increasing from top to bottom. All concentration measurements are subject to total combined uncertainties of <1%. The initial gas temperatures were between 20.5 and 22.5 °C, with the helium-rich layer being generally cooler than the region

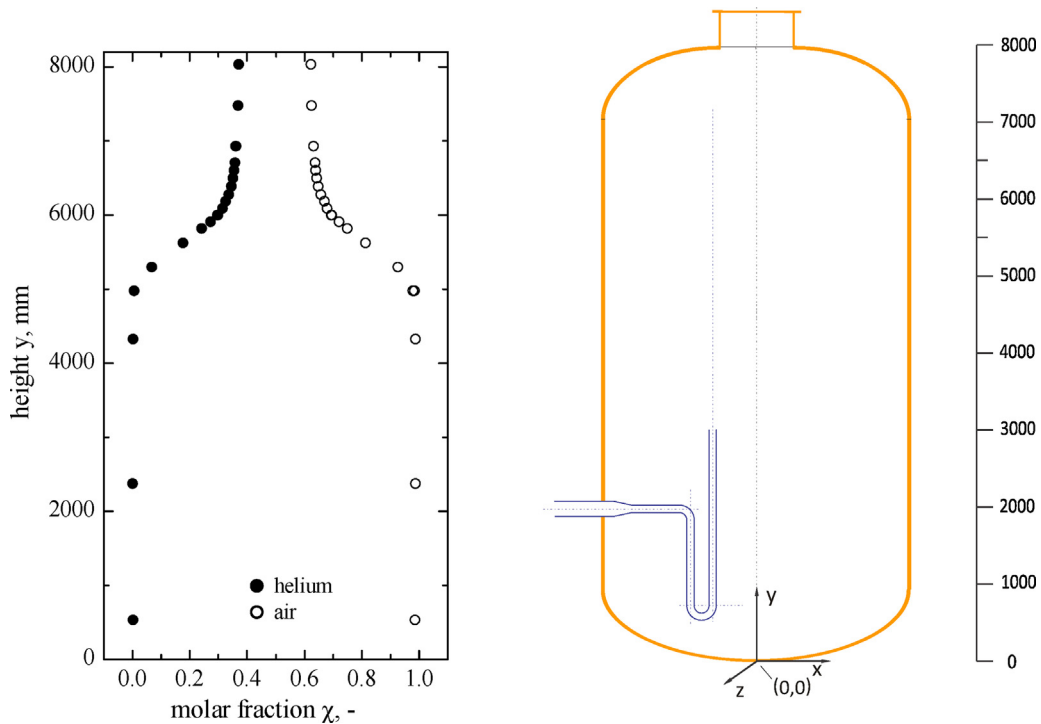


Fig. 2. Initial helium and air concentrations vertical distributions.

below. The wall temperatures were also measured, in the range between 21.6 and 23.2 °C, and all temperature measurements are subject to an uncertainty of ± 0.7 K.

The total volumetric flow rates of helium and air through the injection line have been monitored continuously during the test, and remained constant for the test duration. The mass flow rates of air and helium were 21.52 g/s and 0.42 g/s, respectively. The injected air was not dried before injection into the vessel, and consequently reflects the humidity of the atmosphere at the time of the test. No measurement of the water vapour mass flow rate is available, though the molar fraction measured just above the exit of the injection line (see below) indicates that the water vapour content in the injection was very small.

Injection molar fractions and temperature have been measured 36 mm above the injection line exit. The molar fractions of helium, air and water vapour were constant, at values of 0.134, 0.862 and 0.004, respectively. The temperature increased with time, being initially 20 °C, and rising to 29.3 °C at the end of the transient.

The boundary conditions are summarized in Table 1.

The velocity conditions at the outlet of the injection line were determined in a separate, ex-vessel test; details were given in the technical specifications. They were measured 7.3 mm above the end of the injection pipe, since it was not possible to measure conditions exactly at the pipe outlet. In this ex-vessel test, PIV measurements of the instantaneous values of the Cartesian velocity components (u , v) of the gas mixture emerging from the injection pipe outlet were made. The PIV fields-of-view (FOVs) were taken over the pipe's

internal cross-section in five horizontal planes. From the measured instantaneous velocity components, mean and root-mean-square RMS values of the pipe exit velocity data have been calculated. Details are given in Kapulla et al. (2014a,b). All data have been provided in graphical and tabular form to the benchmark participants.

2.3. Measurements

In this benchmark, selected time-dependent measurements for mass concentration and temperature were made available for comparison. Additionally, the vertical component of velocity, and the RMS values of this component, are also used for the comparison between measurement and calculation at specific times along specified horizontal and vertical lines.

Two mass spectroscopy (MS) instruments have been utilized. The first (MS1) measures the helium, air and water vapour mass concentrations at the inlet to the PANDA vessel (pipe exit) and at the outlet (exit of the vent line). The sampling period for these two lines is 30 s. The second instrument (MS2) monitors these same quantities at 30 other locations in the vessel. The sampling period for these lines is 226 s. Data at nineteen (19) sampling lines were recorded for this benchmark. The estimated uncertainty in the location coordinates for each sampling point is ± 5 mm in each coordinate direction, and, as stated earlier, that for the He concentration measurement is at most 1%.

The K-type thermocouples (TCs), each of 1.0 mm diameter (frequency response 0.5 Hz), have been placed at strategic locations in the PANDA vessel relevant to this test, many in the jet plume issuing from the injection pipe. Temperature measurements have been taken at 218 locations, though only selected temperature data are requested here. The estimated uncertainty in the location coordinates for each TC is ± 5.0 mm in each coordinate direction, and that for the temperature measurement is ± 0.7 K.

Velocities and velocity fluctuations have been measured using PIV in three regions of the flow (see below), all above and around the axis of the injection pipe. These measurements have been processed to produce averaged values over a time period of 204.6 s.

Table 1
Boundary conditions.

Pressure	0.994 bar
Air mass flow rate	21.52 g/s
Helium mass flow rate	0.42 g/s
Gas molar fractions in the inlet flow gas mixture	Air: 0.862 Helium: 0.134 Water vapour: 0.004
Injection temperature	From 20 to 29.3 °C

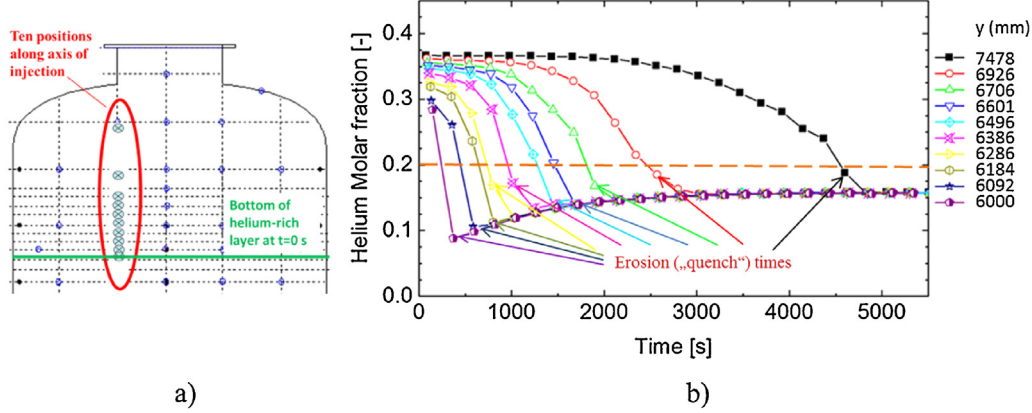


Fig. 3. Positions of concentration measurements used for evaluating the stratification erosion (a) and time histories of helium concentration at those positions (b).

2.4. Calculated variables to compare with experimental data

The main interest of the exercise was to evaluate the capability of the codes to simulate the:

- (a) erosion velocity of the helium-rich layer and
- (b) global mixing in the vessel.

The erosion process is described by the sequential drop of helium concentration below a specified value at increasing elevations along the injection line: this value was chosen to be 0.2. Ten sampling lines locations were chosen to characterise the history of the mixing above the injection. These positions are shown in Fig. 3a.

The time histories of the measured helium concentrations at these locations are shown in Fig. 3b, where the “quench” times are also indicated. As the scanning time was 226 s, the uncertainty of the “quench” times is negative (-226 s), as the reduction below 0.2 can only occur earlier.

The global mixing can be evaluated considering the time history of the helium concentrations at measurement positions distributed over the entire vessel, including some along the injection line. Fig. 4a shows the positions of the measurements used in the present benchmark test. Among the many temperature measurements only five have been selected for the benchmark (Fig. 4b). Four temperature measurements were used to characterise the temperature decay along the axis of the jet, and one (slightly off-axis) to

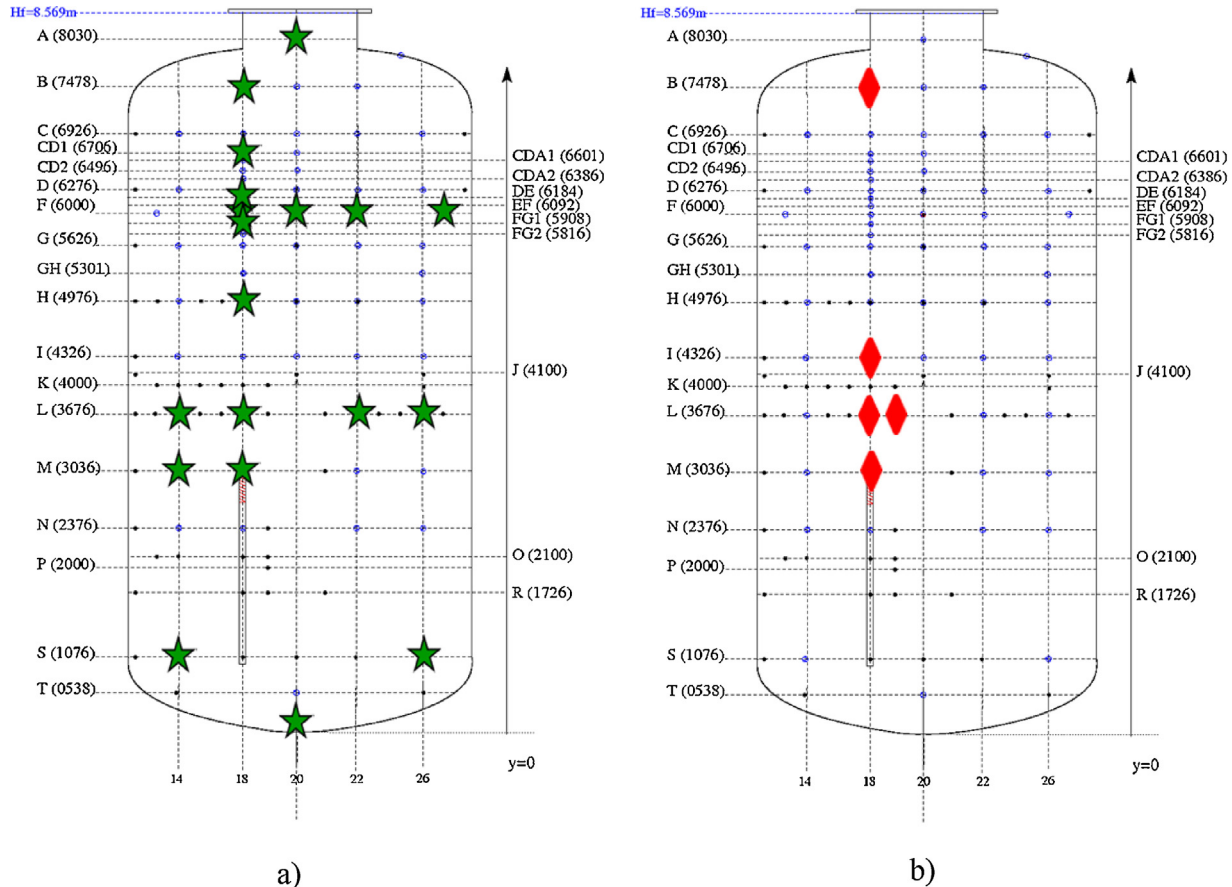


Fig. 4. Positions of: concentration measurements used for evaluating the global mixing (a) and temperature measurements used for the benchmark (b).

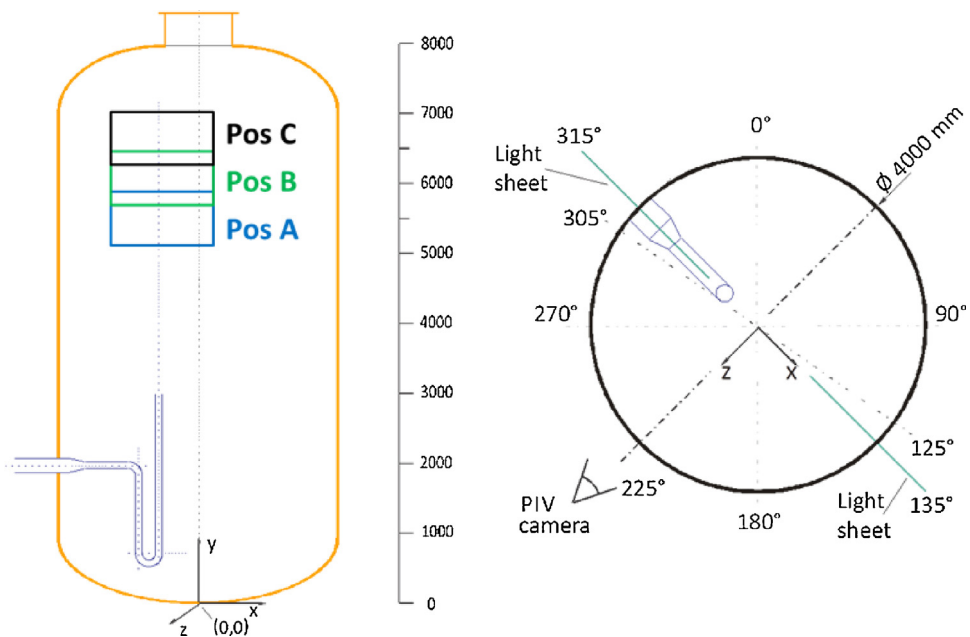


Fig. 5. Positions of the PIV field-of-views (FOVs).

characterise the transversal distribution at short distance from the pipe exit. The comparison of the calculated results with the data was expected to show the capability of the models to properly represent the transversal diffusion and thus the broadening of the jet.

Additionally, seven vertical and horizontal profiles of the mean vertical velocity and the RMS of the vertical velocity fluctuations were requested at three times, to be compared with the values measured by PIV in windows (field-of-views) at three positions (A, B, and C in Fig. 5). The vertical distributions of turbulent kinetic energy (TKE) along the injection axis at three times were also requested, although these variables were not intended to be used for the rankings. Nevertheless, it will be shown below that the comparison of the TKE vertical distributions will be very useful for a first tentative interpretation of the reason for the differences between various simulations results.

3. Summary of the submissions and main results

3.1. Summary of the submissions

Nineteen submissions have been received. They are summarised in Table 2. The entries only address the main features of the physical models, mesh and simulation times. The few details on the numerical methods used that were asked for are not included, but could be considered in the final synthesis report. In general, nearly all simulations used second-order space differencing. Some of the users, however, used first-order differencing in time, and these submissions are among the “worst”. Without a sensitivity analysis, however, it is not possible to correlate the poor predictions with the selected time differencing method, and this issue will not be further addressed in this report.

It is noted that:

- Mostly commercial codes (CFX, FLUENT, STAR-CD) were used. A few submissions used “in-house” CFD codes, and two used a containment code with CFD capabilities (GOTHIC). Finally, only one participant used an open source code (OpenFOAM).
- None of the meshes used are impressively fine. The number of cells ranges between 4000 and 4.3 millions. Since sensitivity

studies were not part of the benchmark exercise, it is not possible to judge whether the nodalisations are sufficiently detailed to fully represent the physical processes modelled. It is left to the individual users to further clarify this important point. Especially for simulations using LES for representing turbulence, the use of large cells should be critically evaluated.

- Approximately half of the participants used standard URANS turbulence modelling approaches, i.e. variants of the well-established $k-\epsilon$ model, in connection with a mesh that aims to resolve the prevailing flow structures (between 400,000 and 2.2 million cells). The other half used refined turbulence modelling (LES, SAS, RSM) or standard modelling on a coarse mesh. For clarity of presentation the contributions in these two classes of submissions (“with standard turbulence modelling” and “others”) are grouped together in the following presentation of the main results.
- Nearly all participants could complete the simulation (7200 s), although at the cost of very large “equivalent” CPU time (referred to a single processor), which for LES simulations would amount to several years on a single processor in spite of all simplifications adopted for this benchmark exercise. These numbers, together with the fact that some users could not complete the simulation, shows how demanding the simulation of a typical flow of interest for containment applications still is. The still too high costs of CFD with a large mesh and long simulation times rises the interest to evaluate the performance of methods used with much coarser meshes.
- The modelling of the pipe and the flow outlet conditions is quite different in the various simulations. In a few simulations the flow inside the pipe is considered (YES in the table) and the measured velocity profile and turbulence intensity at the outlet is reproduced by appropriate choice of the pipe inlet conditions. In most simulations the flow (with prescribed velocity profile) is injected at the level of the injection line exit, where the obstruction of the pipe below is considered (Y/N in the table) or not (NOT in the table). As regards the average turbulence intensity at the pipe outlet, this varies in a surprisingly broad range, between 0 and 20%. Considering the spread of the results for some variables portraying the spatial evolution of the flow above the injection, it is

Table 2

Summary of the submissions (grey shaded: Group 1 submissions, using variants of the $k-\epsilon$ model and a sufficiently detailed mesh; not shaded: submissions, using other turbulence models or a very coarse mesh).

User	Code	Turbulence model	Nr. cells $\times 10^3$	Gas to wall heat transfer	Sc_t	D_{AB} (m^2/s) $\times 10^{-5}$	Inlet pipe		Simulation time (s)	Equivalent CPU time (h)
							Modelled (wall/fluid)	Tu Outlet (%)		
1 ^{*,o}	Trio.U 1.6.8	$k-\epsilon$	2900	No	0.7	7	No	7	2100	105,800
6 [#]	P ² REMICS	$k-\epsilon$	1383	No	1	7	No	10	7535	3024
8	CFX 14.5	SST	717		1	N/A			6981	13,444
11	CFX 15	$k-\omega$ SST	2200	Yes	0.9	7.2	Yes	8	5272	4960
12 [#]	FLUENT 14	RSM	2077	No	0.7	7.13	No	5	7200	1800
17	FLUENT 14.5	$k-\omega$ SST	2200	Yes	0.7	7	N/Y	5	7200	576
19	STAR-CD 4.20	Low-Reynolds $k-\epsilon$	2064	No	0.9	6.7	Yes	8	7200	68,608
20 ^O	CFX-14.5.7	$k-\omega$ SST	1612	Yes	0.9	Correlation	Yes	5 ⁺	4437	20,164
32	FLUENT 12.1.2	$k-\epsilon$ (realizable)	474	Yes	0.7	8	N/Y	13	7200	6960
33	CFX 14.5	SAS-SST	1263	Yes	1	=bulk viscosity		7.3	8000	11,680
34	CABARET 2.5	ILES	4331	No	N/A	1.83/1.86	No		7200	49,152
37	OpenFOAM 2.1.1	Modified $k-\epsilon$	2035	No	1	Correlation	No	1.56	10,500	258,048
38 ^{**}	Logos 4.0.7	Laminar	300		N/A	N/A			~3000	N/A
39	CFX 14.5	SAS-SST	1203	No	0.9	7.2	Y/N	5	7200	7392
41	FLUENT 15	$k-\epsilon$	448	No	0.7	2.88	Y/N	11.8	7200	6600
42	FLUENT 15	LES (dyn. Smagorinsky)	790		0.7	Kin. theory	Yes	N/A	7200	118,440
43 ^{*,o}	FLUENT 14	ZLES/WALE	1626	Yes	0.7	Kin. theory	Yes	20	2000	145,152
45	GOTHIC 8.0(QA)	$k-\epsilon$	4	No	0.7	2.88		0	7000	3
47	GOTHIC 8.0(QA)	$k-\epsilon$ in jet region, Mixing length elsewhere	8	No	(1)	0	No	0	7200	48

* Simulation not complete.

** Very few results submitted.

Results for the times at which helium concentration dropped below 0.2 are incomplete (helium concentration at the top position did not drop below 0.2 within simulation time).

[†] Simulation stopped shortly after the time of the helium concentration drop at position B-18. Results for the other elevations incomplete.

⁺ At the pipe inlet (2 m).

^o RMS values of velocities not provided.

suggested here that the representation of the pipe and the flow exit conditions should be carefully considered in further parametric studies.

- The values of the Turbulent Schmidt number ranged between 0.7 and 1. Since the best value for the kind of flow addressed here is disputed, it can be suggested here that future sensitivity studies should include this parameter. We recall that Sc_t controls the steepness of the density gradient in the mixing zone, and is therefore an important parameter in the simulation of the erosion process.
- Nearly all participants used values for the molecular diffusivity close to $7 \times 10^{-5} \text{ m}^2/\text{s}^2$, which is mostly quoted in technical literature. Four users, however, used smaller values or zero. For these submissions, the role of unwarranted values should be evaluated.
- Many users did not consider heat transfer between gas and the vessel walls. Since the temperature differences within the fluid domain are very small (less than 10 K), it is reasonable to assume that the modelling of the heat transfer did not affect the evolution of the helium concentrations and velocities. Nevertheless, the results submitted for temperatures are invalid, because of the slow warming of the fluid in the entire vessel.
- Nearly all submissions using variants of the $k-\epsilon$ model included the RMS of the vertical velocity calculated from the turbulent kinetic energy, assuming isotropic flow. One submission (U20) did not include these derived variables.

The table does not include any entry related to the use of full buoyancy treatment in the turbulence equations, which is known to affect the mixing of a stratified ambient. Since all participants that responded to a specific enquiry confirmed that buoyancy terms were fully considered, it is assumed that this is true for all simulations (apart, obviously, U38, which used laminar flow assumption),

and differences do not arise from neglecting buoyancy effects on turbulence.

3.2. Main results for all submissions

In this paragraph, the main results for all submissions are compared with the experimental data up to 4000 s (time when the helium concentration at the uppermost elevation along the injection line dropped below 0.2). The results, for clarity of presentation, are subdivided in two groups, namely the results of simulations using variants of the $k-\epsilon$ turbulence model and typical "CFD meshes", and the "others". The simulations are labelled according to user number, turbulence model used, and number of cells adopted (millions). Submission U38 included only a few results, and therefore this contribution will not appear in the comparison plots.

Fig. 6 shows the times at which the helium concentration drop below 0.2 at the selected ten elevations along the injection axis. For both groups of calculations the spread of the results is astonishingly large. It is worth noting that:

- One simulation (U33) predicts the erosion times nearly perfectly. Three simulations (U6, U37, U12) do not calculate the drop at the highest elevation within the simulation time, and two (U8, U34) strongly overpredicts the time of this occurrence (which the two participants extrapolated from the time history of the concentration, and can thus be even larger than that shown in the figure). The upwards penetration of the jet is too slow. All others overpredict the mixing to various extents.
- The variety of results obtained with variants of the $k-\epsilon$ model (Fig. 6a) is quite large. It is especially interesting to note that one of the simulations (U17) using the SST turbulence model

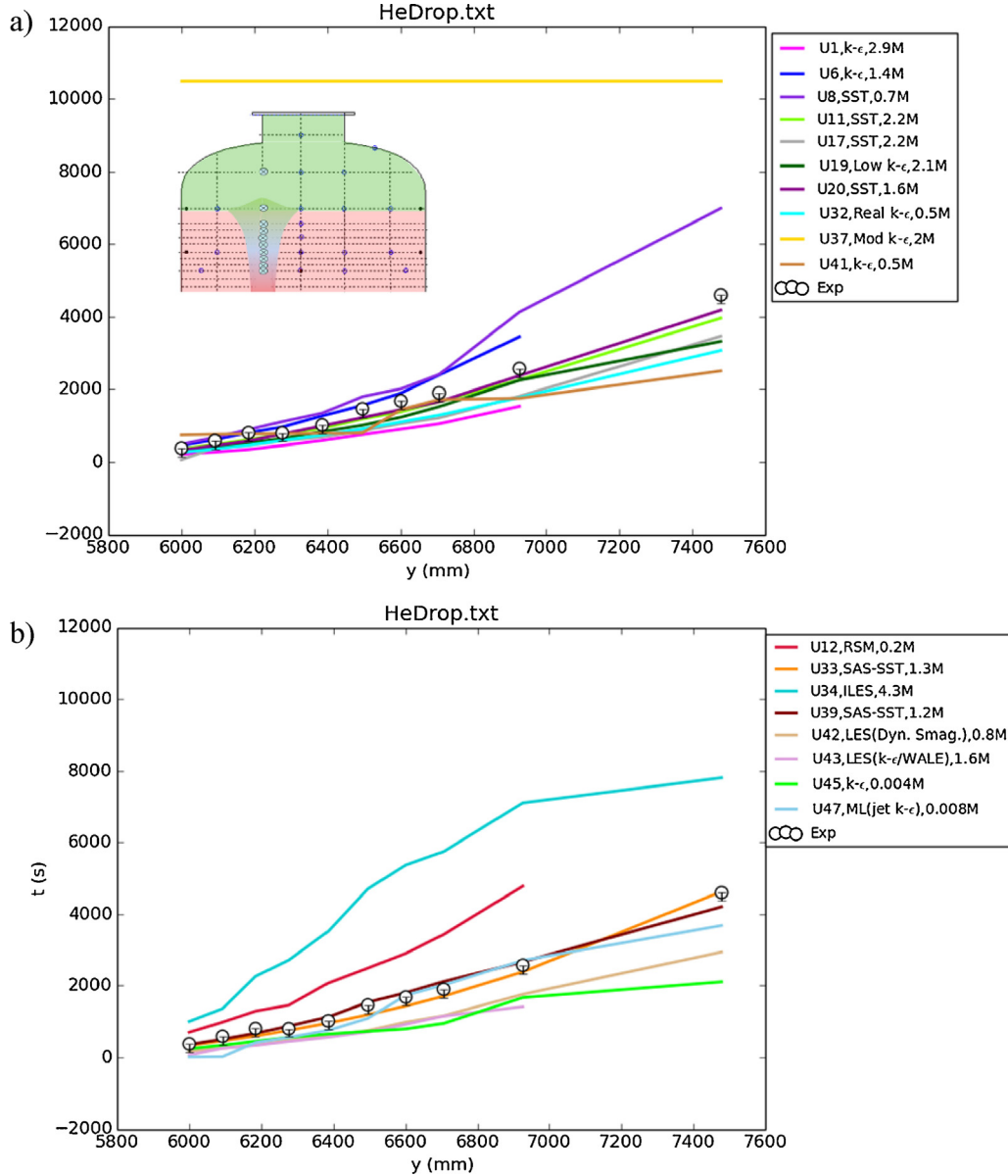


Fig. 6. Times of helium concentration drop below 0.2 at various elevations along injection line: (a) Group 1; (b) Group 2 (see Table 2).

produces results notably different from other two simulations U11 and U20, which use the same turbulence model and meshes of similar detail (from 1.6 to 2.2 million cells). It should be noted that the two best results (U33 and U11) based on all results (see discussion in Section 4.5) were obtained using the CFX code. It would be interesting if a user could run the simulation with the same model choices and mesh, but with the two codes (CFX and FLUENT), to check whether certain results could depend on the solver used (and the way the “control volume” is defined in the two codes) and/or numerical parameters selected. Actually the FLUENT calculation (U17) used default convergence criteria, and some “rugged” curves for other variables (see below) could indicate convergence problems. It is possible that actually the short simulation time reported by U17 was achieved at the cost of reduced accuracy.

- Although the most accurate simulations used the SST and the SAS model, it is not obvious that they should be considered superior to the standard $k-\epsilon$ model, because this latter model was either used in association with a coarser mesh or in the framework of in-house codes, for which the validation is certainly not as extensive

as for commercial codes. Moreover, the participants that submitted the successful results using the SST model were all familiar with previous tests in PANDA.

- All LES simulations produced from poor to very poor results. The use of LES with coarse meshes is rather questionable. These results suggest that accurate simulations for the long transients which are of interest for containment analysis using this advanced modelling are not affordable yet.
- The best predictions seem to be (visual impression will only be partly confirmed by the rankings) obtained by both simulations using the SAS-SST model. It will be shown below that is true for U33 but the good results of U39 in Fig. 6b are misleading.
- Surprisingly enough, very good results (U47) are also obtained with the GOTHIC code and a very coarse mesh (8000 cells). The much worse results obtained by the second GOTHIC user (U45) show the strong dependence of the success of these coarse-mesh calculations on the user effect.

As regards the global mixing, the time histories at two positions outside the jet axis and at the bottom of vessel are considered

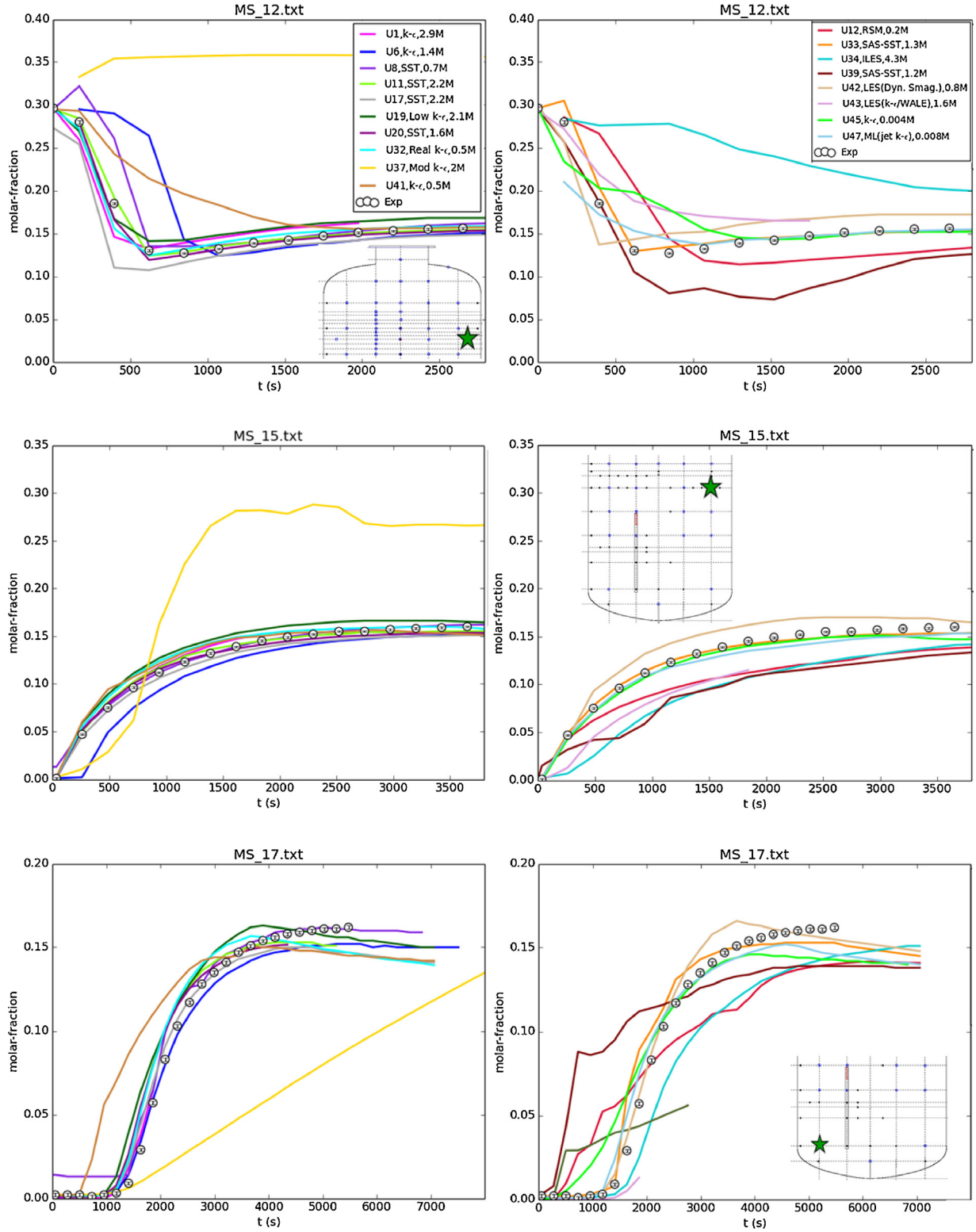


Fig. 7. Helium concentration time histories at two positions outside the jet (top: $z = 6\text{ m}$; middle: $z = 3.676\text{ m}$) and near the vent inlet (bottom).

for illustrating qualitatively the performance of the various codes/models. Fig. 7 shows the calculated and the experimental results for the two groups of simulations. Most simulations using variants of the $k-\epsilon$ model predict reasonably well the mixing outside the jet, and the time of propagation of helium down to the vent. Only one submission (U37) displays completely wrong results, and one user (U41) obtained good agreement at some

positions and large discrepancies at other locations. In particular, U41 predicted too early propagation of helium into the lower head, showing too fast mixing.

It is interesting to note that the nearly constant value (increasing very slowly) at the bottom of the vessel (Fig. 7, MS_17.txt) in the last period of the transient was captured only by two users (U6, U8), whereas all other simulations show

a maximum followed by slow decrease, which is difficult to explain.

The simulations of the second group show a few interesting results:

- The LES simulations show again very different results, with reasonable agreement only obtained by one user (U42), although this submission overpredicts the equilibrium helium concentrations at all positions.
- One of the two simulations using the SAS model (U33) shows excellent agreement with the test data, although the trend at the lowest elevation is less monotonic than in the experiment. In particular, a sudden delayed increase is observed at the time when helium arrives into the lower head. U33 is also the only submission, among those correctly reproducing the general trend, that captures also the nearly constant value of the helium concentration at the end of the transient.
- The other simulation using SAS, which seemingly well predicted the upper layer erosion process, shows a completely unphysical helium concentration evolution at all three positions. Considering the small differences between the mesh and physical parameters adopted by User U39 and those of U33, it is difficult to guess which are the differences in the simulation set-up that result in so large different results. From the information provided, it results that both participants used second-order methods, but User 33 has stricter convergence criteria than User U39, and ran the simulation on a 64 b machine rather than on one with 32 b precision. The investigation of whether convergence criteria and arithmetic precision can be responsible for the dramatically different results will be an interesting aspect of the analyses which are left to the participants.
- Coarse-mesh simulations seem to be capable to capture the global mixing, with results that are comparable with those obtained with meshes composed of a number of cells between two and three order of magnitude larger.

It should be noted that in the first version of the synthesis (Andreani et al., 2014), the location of the vent (MS_19) was considered, which showed completely unphysical results for some simulations. It was later understood, however, that the local conditions at the vent could be affected by the way the boundary condition was set, as no detailed information was provided on the vent line and its hydraulic resistance. Therefore, in some simulations, instead of a continuous vent flow, a small amount of fluid was intermittently calculated to be sucked from the exit funnel. Because of this spurious effect, the results for location MS_17 are considered more representative of the actual performance of the codes, and are thus included in this revised version of the synthesis. It is left to the participants to evaluate whether the inappropriate setting of the boundary condition could have had an impact on the global simulation.

The differences in the calculated erosion rates can partly be explained by the different space evolution of the vertical velocity at the requested times. Since the experimental jet is not perfectly centred with respect to the injection axis and the limited results requested do not permit to derive any information on jet non-symmetries in the simulations, the comparison has to be taken with some caution, also because the experimental data are velocities averaged over about 205 s. Moreover, since in the long term the rate of erosion and the associated re-distribution of helium also affects the composition of the ambient where the jet flows before reaching the density interface, the only meaningful comparison is at the early stage of the transient, when the gas distribution is still close to the initial one.

Fig. 8 shows the vertical distribution of the y -component of the velocity along the injection axis at $t=111$ s, in the region of the

PIV window (Pos. A, between 5009 and 5615 mm). At time $t=111$ s, considering that the helium concentration distribution did not have the time to change much, the PIV window can be assumed to be fully immersed in the transition region, where the helium concentration increases from values close to zero to about 20%. It is thus reasonable to assume that at this early time the velocity at the bottom of the PIV region should be close to that for a free round jet. Indeed, considering that the centreline velocity U_c of a round jet decays according to the equation (e.g., Rajaratnam, 1976; Mi et al., 2001):

$$\frac{U_c}{U_j} = \frac{K_u \cdot d}{(y - y_0)}$$

where U_j is the average exit velocity (=4.67 m/s), y_0 is the virtual origin, and K_u is a constant, the use of values from literature for K_u (between 5.4 and 6.5 for long pipes, see e.g., Rajaratnam, 1976; Mi et al., 2001) results in a value of U_c for a free jet at 2000 mm from the exit of the pipe between 0.95 and 1.26 m/s. The measured value of about 1 m/s thus seems to confirm that initially the jet behaves as a free, round jet.

Therefore, it is quite surprising that only one submission of the first group (U19) accurately predicts the vertical velocity at the bottom of the PIV window, whereas most of the other simulations that were successful in predicting the erosion rate (Fig. 6) underpredict the velocity. It is also noted that the largest discrepancy amounts to about 40%, which for CFD simulations of a free jet is an unexpected result. For this group (with the exception of U11, for which the discrepancy for the velocity is quite large), a correlation exists between the fidelity in predicting the velocity decay and the success in predicting the erosion rate. The simulations of the second group show a similar dispersion of results, with the two submissions using the SAS model and the two using LES with subgrid model reproducing the correct trend and predicting the velocity at the top of the PIV window fairly well. One of the coarse-mesh simulations (U47) also produces comparably good results, whereas the simulation with ILES, RSM and the other coarse-mesh simulation badly fail to predict the correct velocities. Also in this case a correlation exists between the success in the prediction of the erosion rate and the prediction of the jet velocity for all calculations but for the two using LES, which underpredict the upward penetration of the jet in the helium-rich layer, although the approach velocity is slightly over predicted.

A valuable insight in the unexpectedly large variation of results and partly in the root of the contradicting results is offered by the axial evolution of the turbulent kinetic energy (TKE). Fig. 8 shows that, with the exception of U12, the success of the prediction seem to be correlated to the good prediction of the TKE in the PIV region. It can be noted that all LES simulations overpredict TKE due to the coarse meshes used. These results could indicate that the turbulent diffusivity is too large, and the excessive mixing of the incoming jet with the helium-rich layer weakens the jet and delays the erosion. The dispersion of the results, also for simulations using the same model and meshes of the same detail, is again quite impressive, especially considering the near-field region, where, together with well-behaved evolutions, also unphysical trends can be identified, with the position of the maximum outside the expected range (e.g., between 7.5 and 8.5 hydraulic diameters according to Boguslawski and Popiel, 1979). The variety of results in the vicinity of the pipe exit, which indicates that the potential core of the jet has been completely missed in some simulations, strongly suggests that the modelling of the pipe and the implementation of the measured boundary conditions (profiles of velocity and turbulence intensity) may play an important role in determining the capability of the jet to erode the upper layer, and should be considered in the post-test analyses. Due to the similarity of the initial flow

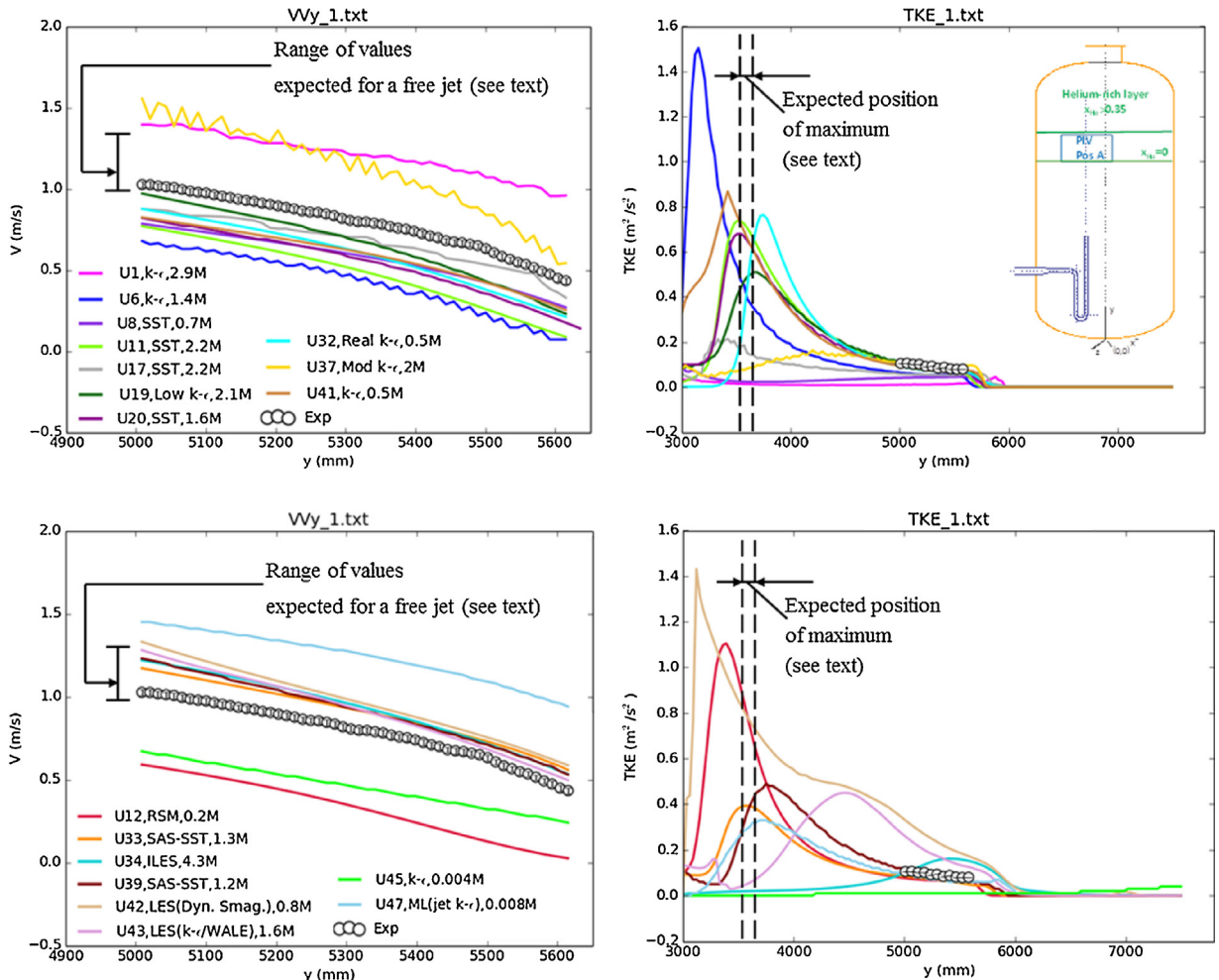


Fig. 8. Vertical distribution of the y -component of the velocity along the injection axis at 111 s (left); vertical distribution of TKE along the same vertical line (right). Top: Group 1; bottom: Group 2 (see Table 2).

with that of a free round jet, it is suggested here that before any full simulation is attempted, the model and all parameters (including the numerical ones) should be checked in separate simulations of the basic flow (free jet). Finally, the rather “rugged” shape of the profiles calculated by some participants could indicate convergence problems and/or the appearance of numerical instabilities.

A final remark about the TKE concerns the trend above the density interface, which was initially the motivation for asking this variable. Consistency prescribes that the TKE decays quickly above the leading edge of the jet interacting with the less dense layer, which “stops” the negatively buoyant jet. Actually this is the case for nearly all simulations. The only submission that shows the unphysical trend of TKE increasing with height well above the density interface is one of the two coarse-mesh simulations (U45). The reason should be investigated.

Some additional general considerations on the fidelity of the various simulations can be gained from the comparison of the calculated results with the two measured temperatures at 3676 mm, which were included in the results to be submitted for this benchmark. Fig. 9 shows the temperatures at two positions at elevation $y = 676$ mm, less than 10 diameters above injection, the first being on the injection axis, and the second at a transversal distance of 325 mm.

It can first be noted that only the simulations that included heat transfer with the wall (Table 2) were capable to reproduce the temperature axial decay from the pipe exit to Level L during

the entire transient. The largest discrepancy, however, concerns the temperature outside the axis (TC5). The simulations that did not consider heat transfer between the gas and the wall show small temperature differences between inside and outside the jet, or even practically the same temperature, which indicates that the entire temperature field inside the vessel was poorly predicted. It is also noted that most of the simulations that correctly predict the temperatures and temperature differences, were also among those that were successful in predicting the erosion rate (U11, U17, U20, U33, U47). The exception is the simulation of U19, which did not consider heat transfer: it is not obvious whether the deviations of the calculated erosion rate from the experimental data in the later phase of the transient could be related to the neglect of this energy transfer mechanism. In general, although it is unlikely that heat transfer played an important role, it can be argued that the choice some users made not to model heat transfer is somewhat unwarranted, and reflects the general issue for any modelling approach (including CFD) to be able to identify the processes of interest for the transients to analyse.

The comparison above provides a full picture of the merits of the various submissions, because the detailed comparison of the PIV results (distributions of velocities and RMS of the velocities at the requested times) is only meaningful for simulations that approximately captured the progression of the upwards displacement of the bottom of the helium-rich layer. These results will be shown in Section 5 only for the “good” submissions, after the

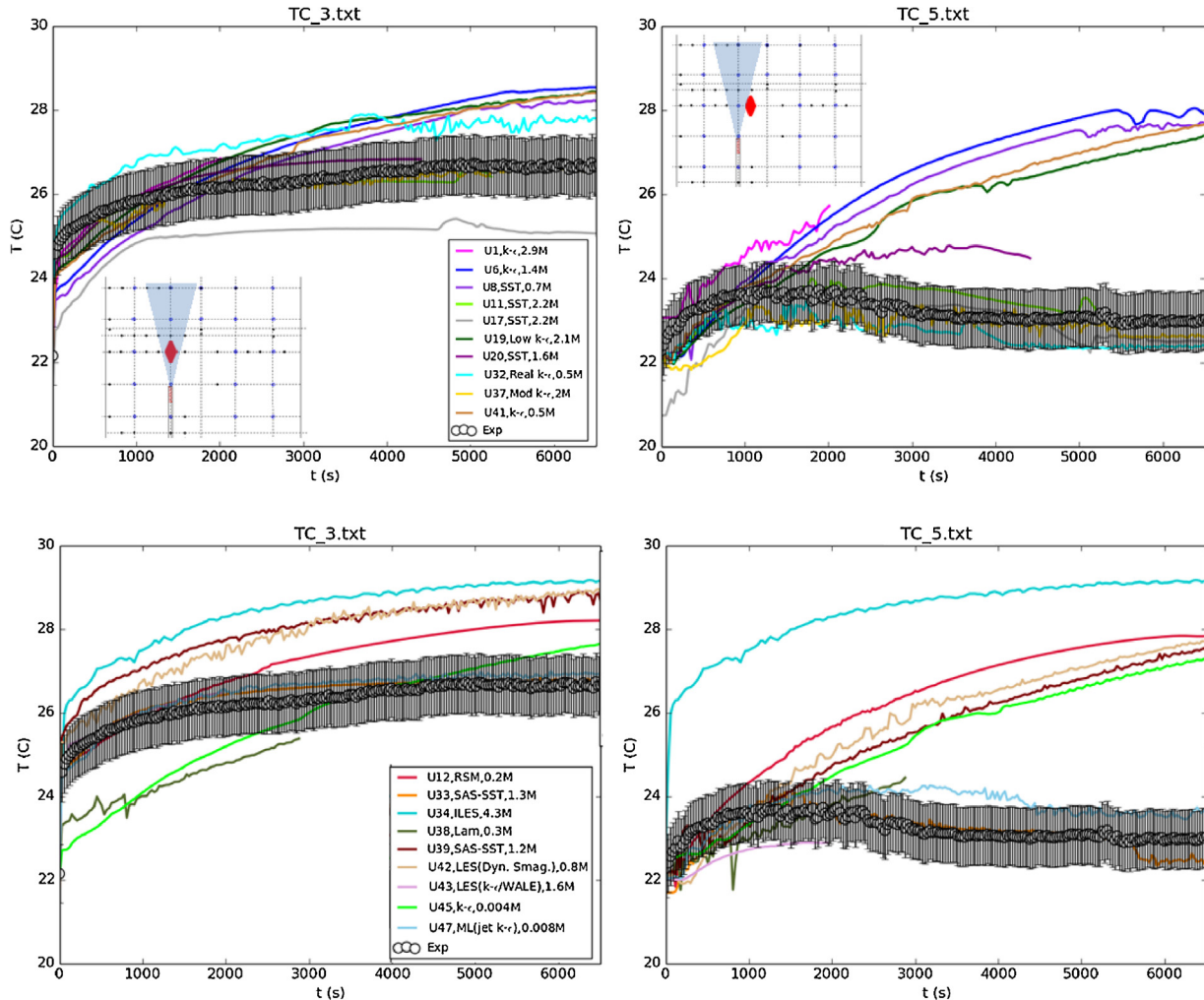


Fig. 9. Temperatures at two positions at $y = 3676$ mm.

ranking according to quantitative comparisons of the calculated results with data is presented in chapter 4.

4. Ranking of submissions

Following the procedure established in the previous two benchmark exercises, a ranking of submissions is produced. Due to large number of variables considered, the ranking based on summary scores (used for IBE-1, Mahaffy, 2010) was preferred to many rankings based on individual scores (used for IBE-2, Lee et al., 2012). The process of ranking was in general made difficult by the circumstance that many submissions were not in compliance with the requested format, simulation time was not the same, in some simulations the helium concentrations at highest elevations did not drop below 0.2 within the simulation time, and some points or entire data files were not provided. Additionally, by the very nature of a transient calculation, certain comparisons may be not meaningful (e.g. horizontal velocity distributions at prescribed times), because some variables at later times suffer from the errors in the prediction of the progression of the leading edge of the jet accumulated during the transient. Finally, the “global ranking” and the penalisations adopted are arbitrary. However, it will be shown below that the quantitative evaluation of the results provides the same ranking that one would make on the basis of the visual inspection of the few results displayed in the previous section. In accordance

with the practice established in the two previous benchmark exercises, the ranking is based on simple linear metrics, with different corrections adapted to the various variables.

4.1. Ranking by comparison with helium layer erosion time

For the ranking of the times when the helium concentrations drop below 0.2, the following formula was used to obtain the score:

$$M_{HD} = \frac{1}{N_p} \left(\sum_{i=1}^{N_I} |C_i - D_i| + \max(|C_i - D_i|) \times (N_p - N_I) \right) \times \frac{\Delta y_{\text{exp}}}{\Delta y_{\text{calc}}} \quad (1)$$

where C_i and D_i are the calculated and experimental values, respectively. The number of points N_p is the total number of experimental points, whereas N_I is the number of calculated points provided. The length Δy_{exp} is the elevation difference between the first and last point, whereas Δy_{calc} is the range of y for which results are provided. Interpolation and/or extrapolation of the participants results was not carried out, and therefore two penalisations for incomplete submissions were adopted: the first affected the incomplete files ($N_I < N_p$) and the second the simulations terminated before the helium concentration at the highest location occurred. For one

Table 3

Ranking by comparison with times of helium concentration drop below 0.2 along injection line.

Ranking	User	Score	Code	Turbulence model	Number of cells (thousands)
1	39	132.13	CFX 14.5	SAS-SST	1203
2	33	142.37	CFX 14.5	SAS-SST	1263
3	11	222.19	CFX 15	k- ω SST	2200
4	47	343.71	GOTHIC 8.0(QA)	k- ε in jet region Mixing Length elsewhere	8
5	20*	345.54	CFX-14.5.7	k- ω SST	1612
6	19	377.95	STAR-CD 4.20	Low-Reynolds k- ε	2064
7	41	483.03	FLUENT 15	k- ε	448
8	17	524.45	FLUENT 14.5	k- ω SST	2200
9	32	524.45	FLUENT 12.1.2	k- ε (realizable)	474
10	6	559.69	P ² REMICS	k- ε	1383
11	8	603.45	CFX 14.5	SST	717
12	42	638.48	FLUENT 15	LES (dyn. Smagorinsky)	790
13	45	732.85	GOTHIC 8.0	k- ε	4
14	1*	979.55	Trio_U 1.6.8	k- ε	2900
15	43*	1040.2	FLUENT 14	ZLES/WALE	1626
16	12	1259.63	FLUENT 14	RSM	2077
17	34	2576.65	CABARET 2.5	ILES	4331
18	37	8921.55	OpenFOAM 2.1.1	Modified k- ε	2035
19	38	N/A**	Logos 4.0.7	Laminar	300

* Penalisation factors applied.

** Results not submitted.

submission (U6) the final missing point was replaced by an extrapolated time considering the provided time-history at the uppermost elevation, which indicated that the helium concentration drop at that elevation did not occur until the end of the simulation. **Table 3** shows the results for the ranking resulting from the application of Eq. (1). Only four submissions were affected by the penalisations. The quantitative ranking confirms the visual impression that the two simulations using the SAS model are the best. It was shown in the previous chapter that for User39 this result is misleading. The table also shows that the SST model, used with CFX and a detailed mesh, was also very successful. The same model used with FLUENT seem to produce less accurate results. The coarse-mesh simulation of User47 is surprisingly ranking fourth.

4.2. Ranking by comparison with all helium concentrations time histories

Also for the comparison of concentration time histories some corrections to the simple metrics were adopted, because the simulation times were different, and there was no reason for penalising simulations at times after the equilibrium value was reached. Therefore, for all submitted results that did not reach the end time

of the experimental data the average discrepancy for the last 4 points was added to the cumulative error for the points supplied. For each individual curve, the following formula was used:

$$M_{C,k} = \frac{1}{N_{P,k}} \left(\sum_{i=1}^{N_{I,k}} |C_{i,k} - D_{i,k}| + \text{avg}(|C_{j,k} - D_{j,k}|)_{j=N_{I,k}-3, N_{I,k}} \times (N_{P,k} - N_{I,k}) \right); \quad k = 1, N_k \quad (2)$$

The global ranking for concentrations was produced considering the sum of the scores:

$$M_C = \frac{1}{N_k} \sum_{k=1}^{N_k} M_{C,k} \quad (3)$$

The ranking resulting from the use of Eqs. (2) and (3) is shown in **Table 4**. The results for the global mixing are quite different from those obtained for the helium layer erosion. The two submissions using CFX and the SST model are the most accurate, followed by the

Table 4

Ranking by comparison with helium concentration time histories at all positions.

Ranking	User	Score	Code	Turbulence model	Number of cells (thousands)
1	20*	0.006368	CFX-14.5.7	k- ω SST	1612
2	11*	0.00689	CFX 15	k- ω SST	2200
3	33	0.007225	CFX 14.5	SAS-SST	1263
4	8	0.009779	CFX 14.5	SST	717
5	17	0.010701	FLUENT 14.5	k- ω SST	2200
6	32	0.01243	FLUENT 12.1.2	k- ε (realizable)	474
7	1*	0.012504	Trio_U 1.6.8	k- ε	2900
8	47	0.013217	GOTHIC 8.0(QA)	k- ε in jet region Mixing Length elsewhere	8
9	19	0.013342	STAR-CD 4.20	Low-Reynolds k- ε	2064
10	42	0.016932	FLUENT 15	LES (dyn. Smagorinsky)	790
11	43*	0.02055	FLUENT 14	ZLES/WALE	1626
12	41	0.022966	FLUENT 15	k- ε	448
13	6	0.024746	P ² REMICS	k- ε	1383
14	45	0.024923	GOTHIC 8.0	k- ε	4
15	39	0.025868	CFX 14.5	SAS-SST	1203
16	12	0.026616	FLUENT 14	RSM	2077
17	34	0.038284	CABARET 2.5	ILES	4331
18	38*	0.082866	Logos 4.0.7	Laminar	300
19	37	0.115459	OpenFOAM 2.1.1	Modified k- ε	2035

* Average of errors for the last four points applied to missing points between end of simulation and end of experimental data recording.

simulation of User 33 using the SAS model. The other SAS simulation (U39) drops down the list, which is in accordance to the very poor predictions shown in Fig. 7. Indeed, also the predictions of most of the concentration time histories show unphysical trends, including those for the positions along the injection line, where by coincidence the wrong slopes for the molar fraction decrease curves hit the 0.2 threshold at approximately the right times. It is also noted that the SST model occupies all first five positions in the ranking. The coarse-mesh simulation of User47 drops is the ranking to position 8, but the global results are still acceptably accurate.

4.3. Ranking by comparison with PIV data

The ranking related to PIV data is affected by the incomplete submissions of some participants. In some cases the RMS curves were not supplied, and in the case of short simulations, also the profiles at the last requested time (2550 s) are missing. However, no penalisation was applied to the score of those participants, because the general results are not affected. In a revised version of this synthesis

report, other criteria could be applied.

$$M_{V,kk} = \frac{1}{N_{P,kk}} \left(\sum_{i=1}^{N_{I,kk}} |C_{i,kk} - D_{i,kk}| + \max(|C_{i,kk} - D_{i,kk}|) \right. \\ \left. \times (N_{P,kk} - N_{I,kk}) \right); \quad kk = 1, N_{kk} \quad (4)$$

$$M_V = \frac{1}{N_{kk}} \sum_{kk=1}^{N_{kk}} M_{V,kk} \quad (5)$$

where $N_{kk} = 20$

The ranking resulting from the use of Eqs. (4) and (5) is shown in Table 5. Surprisingly, the simulation using the low-Reynolds $k-\varepsilon$ model is at the top of the ranking. The SAS and the SST simulations are also quite accurate, in accordance with the good predictions for gas concentrations. The second unexpected result, is the good

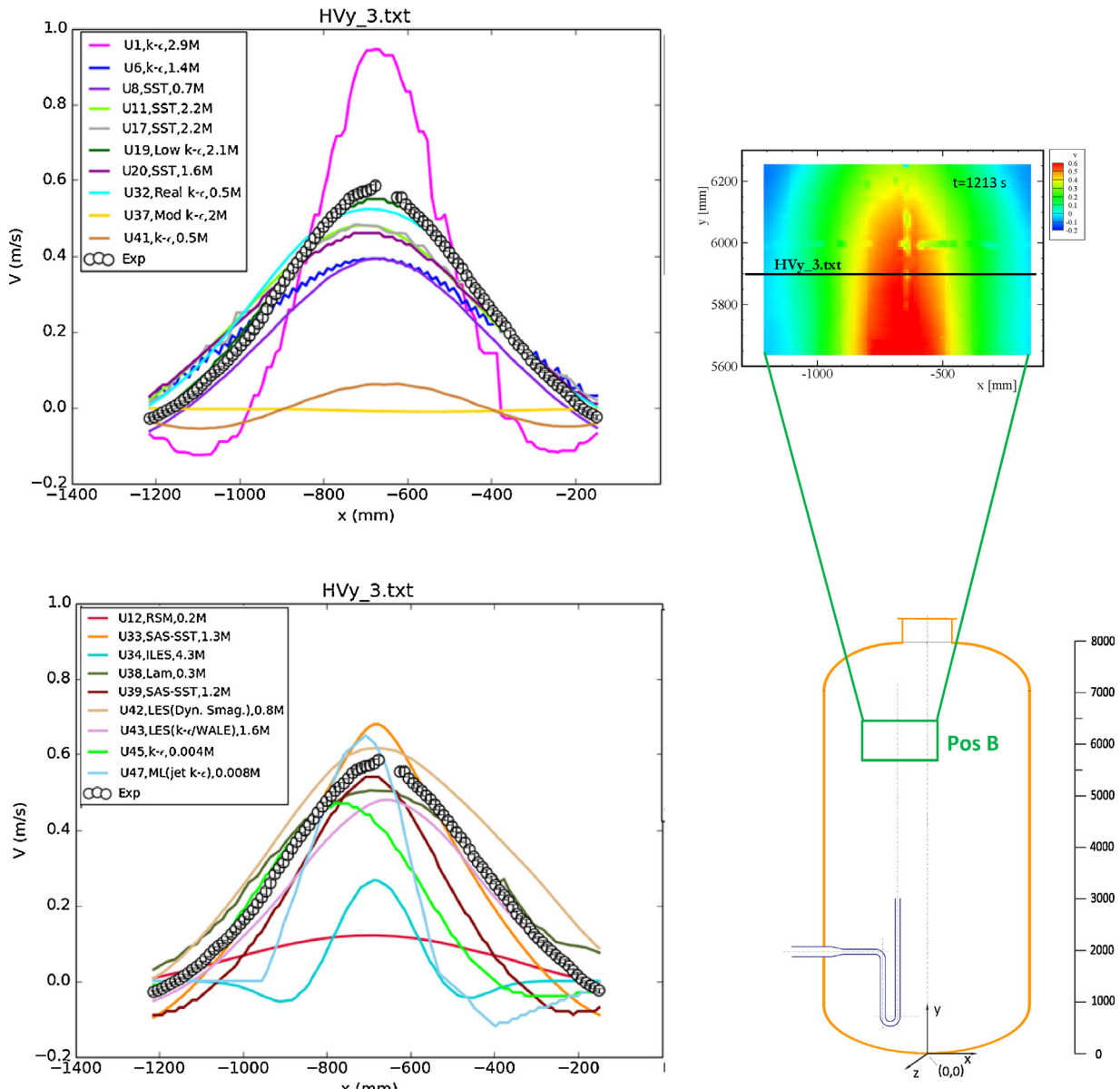


Fig. 10. Horizontal velocity profile in the PIV window at Pos. B at 1213 s.

Table 5

Ranking by comparison with all distributions of velocity and RMS of velocity.

Ranking	User	Score	Code	Turbulence model	Number of cells (thousands)
1	19	0.030864	STAR-CD 4.20	Low-Reynolds k- ε	2064
2	33	0.042677	CFX 14.5	SAS-SST	1263
3	17	0.053371	FLUENT 14.5	k- ω SST	2200
4	11	0.056253	CFX 15	k- ω SST	2200
5	43*	0.069902	FLUENT 14	ZLES/WALE	1626
6	20**	0.085929	CFX-14.5.7	k- ω SST	1612
7	42	0.08851	FLUENT 15	LES (dyn. Smagorinsky)	790
8	41	0.10737	FLUENT 15	k- ε	448
9	6	0.112356	P ² REMICs	k- ε	1383
10	32	0.112795	FLUENT 12.1.2	k- ε (realizable)	474
11	39	0.117372	CFX 14.5	SAS-SST	1203
12	8	0.134797	CFX 14.5	SST	717
13	45	0.136508	GOTHIC 8.0	k- ε	4
14	34	0.157637	CABARET 2.5	ILES	4331
15	38*	0.168391	Logos 4.0.7	laminar	300
16	47	0.19163	GOTHIC 8.0(QA)	k- ε in jet region Mixing Length elsewhere	8
17	37	0.196789	OpenFOAM 2.1.1	Modified k- ε	2035
18	12	0.200418	FLUENT 14	RSM	2077
19	1*	0.238273	Trio.U 1.6.8	k- ε	2900

* Score based on the reduced number of curves submitted.

** RMS of velocities not calculated

Table 6

Ranking by comparison with temperature time histories at all positions.

Ranking	User	Score	Code	Turbulence model	Number of cells (thousands)
1	11*	0.334318	CFX 15	k- ω SST	2200
2	33	0.353955	CFX 14.5	SAS-SST	1263
3	37	0.48333	OpenFOAM 2.1.1	Modified k- ε	2035
4	32	0.537777	FLUENT 12.1.2	k- ε (realizable)	474
5	17	0.568504	FLUENT 14.5	k- ω SST	2200
6	43*	0.600564	FLUENT 14	ZLES/WALE	1626
7	47	0.668245	GOTHIC 8.0(QA)	k- ε in jet region Mixing Length elsewhere	8
8	20*	0.680073	CFX-14.5.7	k- ω SST	1612
9	38**	0.686345	Logos 4.0.7	laminar	300
10	1*	0.912318	Trio.U 1.6.8	k- ε	2900
11	41	1.562964	FLUENT 15	k- ε	448
12	19	1.564045	STAR-CD 4.20	Low-Reynolds k- ε	2064
13	8	1.651109	CFX 14.5	SST	717
14	6	1.672927	P ² REMICs	k- ε	1383
15	39	1.680409	CFX 14.5	SAS-SST	1203
16	12	1.820764	FLUENT 14	RSM	2077
17	45	1.908055	GOTHIC 8.0	k- ε	4
18	42	1.912491	FLUENT 15	LES (dyn. Smagorinsky)	790
19	34	2.737936	CABARET 2.5	ILES	4331

* Average of errors for the last four points applied to missing points between end of simulation and end of experimental data recording.

** Score calculated using the reduced number of curves submitted.

Table 7

global ranking.

Ranking	User	Score	Code	Turbulence model	Number of cells (thousands)	Equivalent CPU time (days)
1	33	0.03239	CFX 14.5	SAS-SST	1263	487
2	11	0.039742	CFX 15	k- ω SST	2200	207
3	20	0.059263	CFX-14.5.7	k- ω SST	1612	840
4	17	0.064848	FLUENT 14.5	k- ω SST	2200	24
5	19	0.069577	STAR-CD 4.20	Low-Reynolds k- ε	2064	2859
6	32	0.080718	FLUENT 12.1.2	k- ε (realizable)	474	290
7	39	0.091630	CFX 14.5	SAS-SST	1203	308
8	47	0.092185	GOTHIC 8.0(QA)	k- ε in jet region Mixing Length elsewhere	8	2
9	41	0.104910	FLUENT 15	k- ε	448	275
10	8	0.105764	CFX 14.5	SST	717	560
11	42	0.108558	FLUENT 15	LES (dyn. Smagorinsky)	790	4935
12	43	0.110651	FLUENT 14	ZLES/WALE	1626	6048
13	6	0.11437	P ² REMICs	k- ε	1383	126
14	45	0.134477	GOTHIC 8.0	k- ε	4	0.15
15	1	0.144330	Trio.U 1.6.8	k- ε	2900	4408
16	12	0.181669	FLUENT 14	RSM	2077	75
17	34	0.276656	CABARET 2.5	ILES	4331	2048
18	37	0.709589	OpenFOAM 2.1.1	Modified k- ε	2035	10752
19	38	N/A*	Logos 4.0.7	Laminar	300	N/A

* Only few results submitted.

performance of the LES simulations using subgrid models. The good results of User 43 are somewhat misleading because are based only on the results at early times, but the results of User 42 show unambiguously that the velocities and RMS of the velocities calculated by LES are by far calculated better than the concentrations. On the other hand, the coarse-mesh simulation of User47 (where the results at all requested points were obtained by linear interpolation) is quite low in the ranking, as expected.

As an example, Fig. 10 illustrates the quality of the various predictions at Position B at $t = 1213$ s.

It can be noted that the simulation U19 (low-Reynolds $k-\epsilon$ model) predicts the velocity profile very well, including the small region of negative values. The velocity distribution is slightly narrower than those predicted by the most successful SST simulations, and therefore closer to the experimental results. This is true for all profiles of vertical velocity and RMS of the velocity. The predictions of U19 are in average better than those of U33 (ranking second), which perfectly predict the outer region of the velocity profiles, but overpredict the peak of the horizontal distribution. Fig. 10 is also a good example of the profiles predicted by U42 and U43 using LES, which are completely different, with opposite deviations from the experimental values. The velocities obtained with the coarse-mesh simulation (U47) exhibit an unphysically narrow profile: at higher elevation and later times the velocities are generally underpredicted.

4.4. Ranking by comparison with temperatures

The comparison of temperatures is only meaningful for those simulations that included the modelling of heat transfer between the gas and the walls. Without considering this phenomenon, the temperature of the entire fluid domain increases, because the long duration of the transient (2 h) makes the small addition of energy due to the warm air injected sufficient to produce a global heat-up. The procedure to calculate the score for this ranking is similar to that used for the concentrations (Section 4.2):

$$M_{T,s} = \frac{1}{N_{P,s}} \left(\sum_{i=1}^{N_{I,s}} |C_{i,s} - D_{i,s}| + \text{avg}(|C_{j,s} - D_{j,s}|)_{j=N_{I,s}-3, N_{I,s}} \right. \\ \times \left. (N_{P,s} - N_{I,s}) \right); \quad s = 1, N_s \quad (6)$$

$$M_T = \frac{1}{N_s} \sum_{s=1}^{N_s} M_{T,s} \quad (7)$$

where $N_s = 5$. The ranking is shown in Table 6, where the top positions are still taken by the SAS and SST simulations, with the

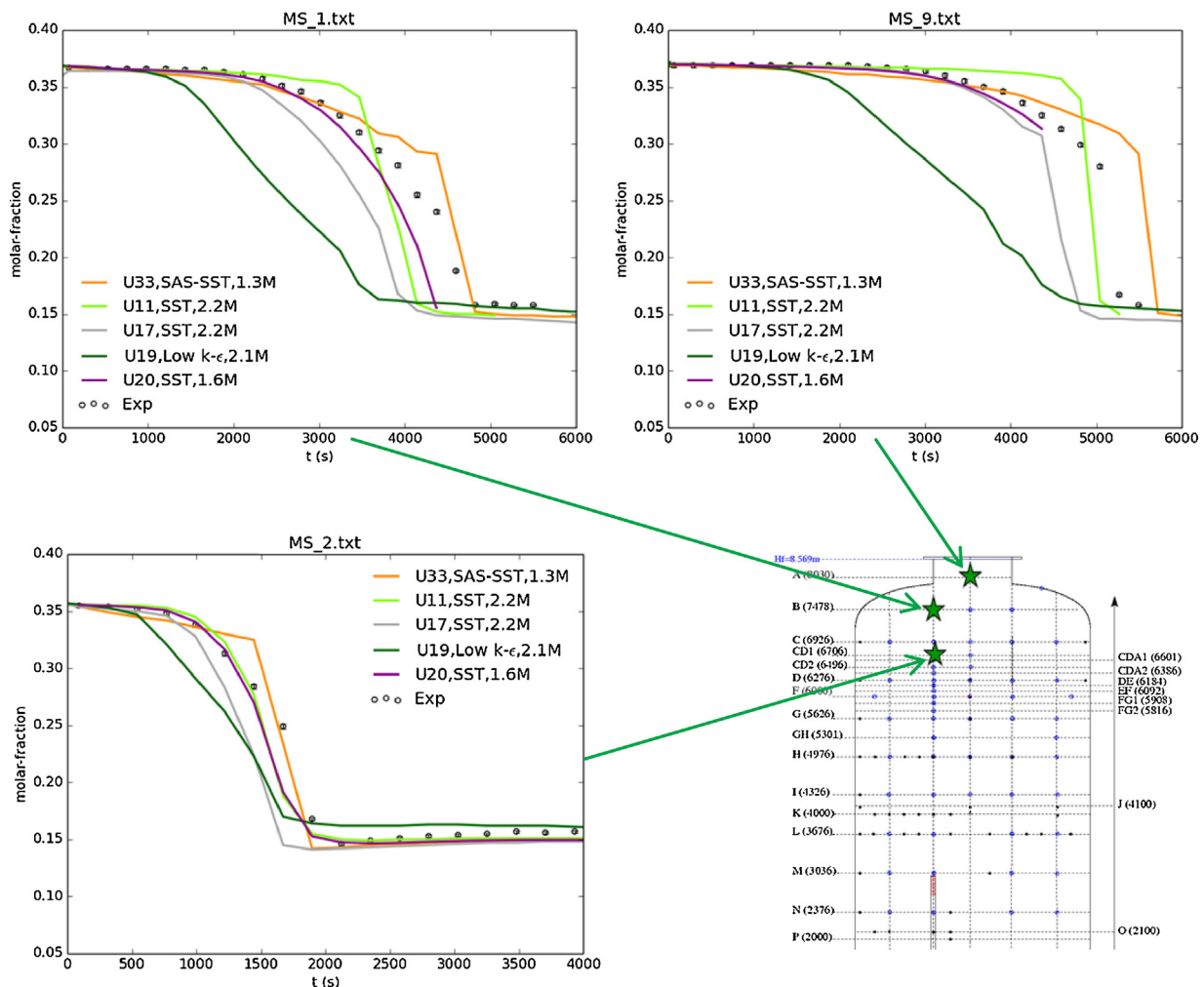


Fig. 11. Helium concentration time-histories at the three uppermost locations considered for the benchmark exercise: A.20 ($y = 8030$ mm); B.18 ($y = 7478$ mm) and CD1.18 ($y = 6706$ mm).

only exception of position 3, which is occupied by simulation (U37) using OpenFOAM and a modified version of the standard $k-\epsilon$ model. Actually, Fig. 9 shows that with respect to temperatures, the predictions of User 37 are quite successful. This must be a pure coincidence, because all other variables were poorly predicted.

4.5. Global ranking

Finally, the global ranking requires a number of arbitrary choices. First of all, the four partial scores are dimensional, and therefore they should be normalised. It was chosen to normalise them using the ranges of variation of the variables. For the helium concentration drop times the range R_{HD} is the time span between the experimental occurrences at the first and last position. For the helium concentration time histories the range R_C is the maximum concentration at $t=0$. For the velocities, the range R_V is the maximum measured velocity. For temperatures, the range R_T is the difference between the maximum and minimum temperatures at the five positions considered for the benchmark. This results in the

following normalising values:

$$R_{HD} = (4597 - 373) = 4224 \text{ s}; \quad R_C = 0.367;$$

$$R_V = 1.026 \text{ m/s}; \quad R_T = (29.25 - 23) = 6.25 \text{ K} \quad (8)$$

The second choice regards the weight factors. Since the erosion progression and the helium concentrations are the most important parameters, the following weight factors have been chosen:

$$W_{HD} = 0.25; \quad W_C = 0.4; \quad W_V = 0.25; \quad W_T = 0.1$$

The global score for each user has therefore being calculated from:

$$M = \frac{M_{HD}}{R_{HD}} \times W_{HD} + \frac{M_C}{R_C} \times W_C + \frac{M_V}{R_V} \times W_V + \frac{M_T}{R_T} \times W_T \quad (9)$$

This procedure results in the ranking shown in Table 7. The first positions are still held by one of the SAS simulations (U33) and three submissions using the SST model, with the two best using the CFX code. A good ranking has also been achieved by the simulation using the low Reynolds number $k-\epsilon$ model and that using

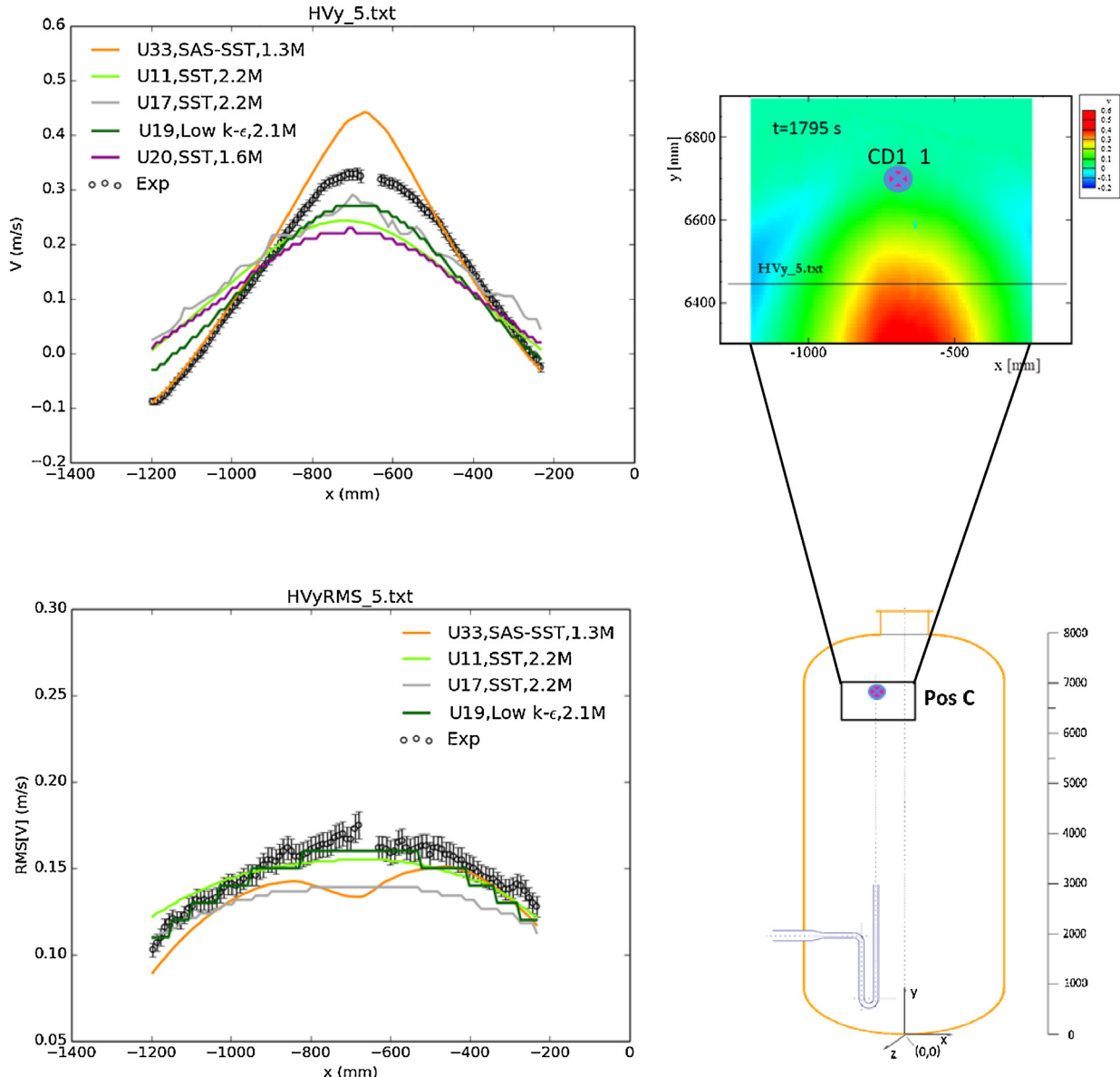


Fig. 12. Velocity and RMS distributions at $t = 1795$ s at $y = 6447.2$ mm, about 260 mm below the position of the concentration measurement CD1.18.

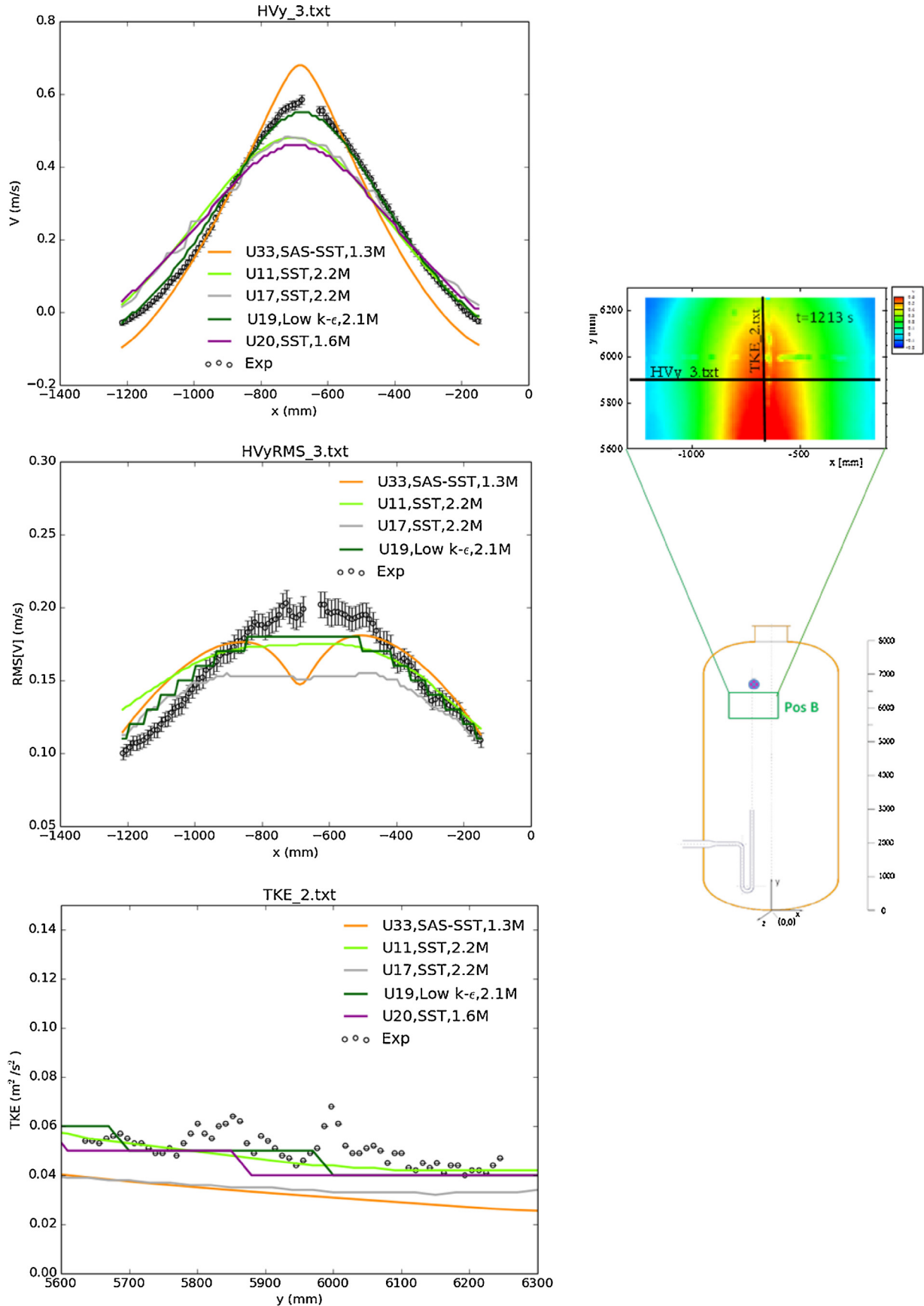


Fig. 13. Horizontal velocity and RMS distributions at $t=1213$ s at $y=5904.1$ mm (about 800 mm below the position of the concentration measurement CD1_18), and TKE vertical distribution at $t=1213$ s.

the realizable $k-\varepsilon$ model. The good position of the second SAS simulation should not be considered because of the unphysical results for some concentrations. It is interesting to observe that the best results using the standard $k-\varepsilon$ model (in conjunction with the mixing length model in the jet region) have been obtained with a very coarse mesh.

The global ranking confirms that the LES simulations were quite unsuccessful, probably because of the need to use a rather coarse mesh (for this kind of simulations), which was the only that could be afforded.

An additional consideration regards the computational costs of the simulations, which in Table 6 is now shown in days of equivalent CPU time. It is observed that the accuracy of the simulations does not correlate with the cost, with quite reasonable results (Rank 4 for U17) can be obtained at still low computational cost. The much larger computation times necessary for the most successful simulation are not due to the use of a particular model (the SAS simulation of User 33 costs less than the SST simulation of User 20), but seems to be linked to the use of a solver (FLUENT) instead of another (CFX). Since the results on similar meshes obtained with CFX are better than those obtained with FLUENT, it would be interesting to understand if a smaller gain of accuracy (possibly due to the choice of different numerical parameters) is only possible at the cost of much larger computation times.

5. Comparison of selected variables for high-ranking submissions

The ranking (as well as visual inspection of the main results) shows that the most accurate simulations predict all variables reasonably well. The only exception is the calculation of User19, which missed the temperatures because it did not consider the heat transfer between gas and vessel walls. Therefore, the temperatures will not be considered in the discussion of certain additional results.

In this chapter only the results of the top five submissions will be compared with the data, addressing in more detail the stratification erosion process.

Fig. 11 shows the helium concentrations at the top three locations for which calculated results have been requested. The uppermost location is just below the man-hole, and is not on the injection axis. First of all, from the time-histories a major qualitative discrepancy of submission U19 becomes apparent. The helium concentration in the dome and immediately below starts decreasing much earlier than in the test, and is much more gradual. This representation of the results emphasises the degradation of the accuracy of the simulation with time progressing. A second consideration can be made regarding the differences between the shapes of the curves predicted by the other simulations. Due to the geometry of the dome, the experimental curve at position A_20 shows a sudden helium concentration drop, which is reproduced by three of the simulations, although at different times, whereas simulation U20 terminates too early. At the lower position B_18 the simulation U33 and U11 predict a sudden drop, whereas the other simulations exhibit a much more gradual decrease. It is interesting to note that the two submissions U11 and U20, so similar in many respects seem to show a different mechanism of erosion of the helium-rich layer at this elevation. At the elevation CD1_18, however, both simulations show a gradual decrease, qualitatively similar to that predicted by User U17. The simulation with the SAS model, instead always predicts sudden drops at all elevations. In the attempt to correlate the different erosion mechanism with velocity and turbulence related variables, horizontal distributions in the vicinity of that location are considered. Fig. 12 shows the horizontal distribution of the vertical velocity and of the RMS of the vertical velocity at about 260 mm below the position CD1_18 where the concentration was measured, at a time ($t = 1795$ s) when the helium concentration had

just dropped below 0.2. It is observed that the velocity distribution calculated by the SAS simulation is more peaked than the others, and the turbulent fluctuations are small compared with U11, especially in the centre, where the distribution exhibits an unphysical depression.

These results seem to indicate that in simulation U33 the erosion process is more strongly driven by the penetration of the jet and less by the turbulent diffusion than in simulations U11 and U17 (which shows small RMS but also smaller velocities). For simulation U20 the RMS of the velocity were not provided and therefore no comparison can be made.

In summary, the inspection of the turbulence quantities brought some better understanding of the differences between the erosion process calculated by top ranking simulations. In particular, the too sharp helium concentration drop predicted by the SAS simulation is related to the smaller values of turbulence in the centre of the jet. The reduced turbulent diffusion is compensated by a higher peak in the velocity profile. The origin of the peculiar shape of the distribution and the question whether it is physically reasonable should be further investigated. Differences between the two SST simulations using CFX and that using FLUENT seem to be related to the smaller turbulence predicted by the latter one. Differences between the two CFX predictions, which are appearing only at some elevations, can only be explained by a more complete analysis that is left to the participants.

Similar differences between the SAS simulation and the other top ranking submission is also observed at a time ($t = 1213$ s) closer to the start of the erosion at the location CD1_18, at a position somewhat lower (800 mm below). Fig. 13 shows the horizontal distributions measured in the PIV window B, which does not include the elevation of sensor CD1_18. At elevation 5904 mm, the differences between the distributions calculated with the SAS model and the others are more evident. Indeed, the velocity distribution is even more peaked than before, and the double-peaked distribution of the RMS is much more pronounced. The other simulations show a practically coincident velocity distribution, and regular RMS distributions. Also at this elevation the RMS for submission U17 are smaller than for the other SST simulations, which is likely to be responsible for the slower erosion, especially at the beginning of the transient. For submission U20, which did not provide the RMS of the velocities, it is interesting to compare the TKE at the same time. It is observed that the TKE is very close to the experimental values and similar to that calculated by U11, which in accordance with the very similar erosion times calculated by the two simulations.

6. Conclusions

The first general conclusion of this benchmark exercise related to containment flows is that even for a simple, basic flow, a variety of results can be obtained, with an unexpectedly large spread of the main variables. In fact, the rate of the erosion of the helium-rich layer was strongly overpredicted by some simulations, but a few simulations predicted the persistence of stratification to the end of the calculated time, which was much longer than the time of the experiment and in some cases exceeded the recommended simulation time. This large spread, growing with time, indicates that the set-up of a new problem (at least for those users that never simulated before a similar experiment in the PANDA geometry) implies the risk of wrong choices, which, possibly can only be avoided by some learning process on similar problems. Hopefully, post-test analyses will identify the reasons for the failure of some simulations and the limited accuracy of most submissions. Since we have no information on the application of the Best Practice Guidelines and the studies on the effect of selecting different convergence criteria (the participants were asked to submit only one calculation), it is not obvious whether the application of these

general recommendations could have reduced the spread of the results. However, it is clear that an established methodology for performing CFD simulations of the long transient of interest for containment safety analyses does not exist yet. In fact, the detail of the mesh used varied in a broad range, and in absence of any accompanying report, it is not clear whether any criterion was used by the individual participant to arrive at the conclusion that the mesh was adequate. Obviously, for turbulence modelling a variety of choices was expected, and the prevailing use of the most popular variants of the $k-\epsilon$ model was also anticipated. However, other modelling choices and parameters were quite different for the various submissions, including modelling of the injection and turbulent Schmidt number. Moreover, the molecular diffusivity was not treated in the same way in all simulations, and the heat transfer between the gas and the vessel wall was considered by only a few users. The cumulative effect of all these choices is difficult to estimate.

Finally, the effect of heat transfer with the walls was only considered by a few participants, which provided the most accurate results. Although the importance of heat transfer can only be quantified by appropriate parametric studies, it is presumed that it should not be neglected for accurately modelling the erosion process. This is an example of how the tackling of a new problem could lead to questionable simplifications and modelling choices.

A few simulations predicted fairly well the transient, and the success of the calculation is not necessarily correlated with the selection of the turbulence model. In fact, although the most accurate simulations used the SST and the SAS model, it is not obvious that they should be considered superior to the standard $k-\epsilon$ model, because this latter model was either used in association with a coarser mesh or in the framework of in-house or open-source codes, for which the validation is certainly not as extensive as for commercial codes. On the other hand, the two predictions using the SAS model produced largely different results, one of them totally missing the global mixing time and predicting migration of helium to the bottom of the vessel after a very short time from the beginning of the transient, thousands seconds before this occurred in the test. Also the fidelity of the predictions with the SST model was different for the three submissions using this model, although mesh, parameters and other modelling choices are apparently close to each other, and the participants using this model were all familiar with previous tests in PANDA. One interesting question which is left to follow-up studies is whether the better accuracy of the two simulations using CFX than that using FLUENT is due to the differences in the solver, or the reason could be the more stringent convergence criteria selected.

It is also interesting to note that the accuracy of one coarse-mesh prediction (U47, who used only 8000 cells) is comparable to that obtained by the best CFD predictions, at least with respect to the mixing of the initially stratified ambient, at a fraction of the computational cost of the most accurate simulations. Although the simulation used a combination of the $k-\epsilon$ model and the Mixing Length model for turbulence modelling, which could be considered bad practice by the CFD community, the results of this benchmark should draw the attention once more to the issue of the reasonable balance between accuracy and computational cost.

As regards the performance of the LES simulations (three submissions), it can be definitely stated that it was far below the expectations, the results being closer to the worst predictions than to the best ones. Since the mesh used was rather coarse for this kind of modelling approach and still the computation times were an order of magnitude larger than for most RANS simulations, the only result of this benchmark in relation to the applicability of LES for containment analysis is that these simulations are not affordable yet for the long transients of interest.

Another interesting result emerging from the comparison of all simulations is the spread in the velocity and turbulent kinetic

energy vertical profile along the injection line, and the limited accuracy in comparison with measured values. The variety of results indicates that the modelling of the free jet is not a trivial component of the global modelling approach. In particular, the comparison of the calculated axial velocity profile with the experimental values at one time where the buoyancy and stratification effects can be considered to be still minimal exhibits a large spread of results. In this respect, it is remarkable that for one of the most successful simulations (according to the global ranking) the discrepancy amounts to about 30%. This result suggests emphasizing the recommendation that any modelling approach should be first validated against basic flows.

Acknowledgements

The experiment was conducted by the experimental group of the Laboratory for Thermal-hydraulics of PSI, composed by G. Mignot, S. Paranjape, D. Paladino, L.Ryan, M. Fehlmann and S. Suter (in addition to one of the authors, R. Kapulla). The exceptional care they used in designing and conducting the experiment and their personal dedication to the commitment to produce CFD benchmark-grade data is gratefully acknowledged. The authors are also indebted to B. Smith for his administrative support within the OECD/NEA CFD activities groups, but also for his technical input to the definition of this benchmark exercise.

Appendix A. Significance of scores and need for better methods to evaluate accuracy of submissions

In this appendix some difficulties in using the linear metrics based on average errors and summary scores for determining the rankings are discussed. These will lead to some basic questions on how to design a method for automatically evaluating the accuracy of a simulation using experimental data and if this information can be used to decide whether a certain computational approach (code, mesh, models, etc.) can be used for the analysis of a similar transient in a real containment. Indeed, the validation of the code against experimental data should serve the purpose to provide a basis for the qualification of the code for a specific application.

It has been shown that the global ranking (Table 7) indicated that the submissions U33, U11, U20, U17 and U19 were the most accurate. It was already shown, however, that submission U19 was affected by a systematic discrepancy with experimental helium concentrations time-histories (Fig. 11), and this important deviation was reflected by the ranking related to the global mixing (Table 4) but not by the ranking related to helium-rich erosion times (Table 3), because the threshold of 0.2 was hit at approximately the right times, although following a wrong trend. But also the middle position of U19 in the ranking in Table 4 would not bring to light the large inaccuracy of the simulation, because an “average” error of 1.33% seems to be quite acceptable.

Considering that the main purpose of the benchmark exercise was to verify to what extent the code can predict the mixing in an initially stratified environment, instead of combining the errors at all positions, the ranking could be made on the base of the evaluation of certain specific “target variables” (similarly to the selected variables in IBE-2). The most obvious candidates for serving as such are the time-histories of the concentration at the top position along the injection axis (MS.1), at the vent (MS.19), and the maximum of the average deviation at all positions. Table A1 shows the deviations for these variables. This shows again that the best predictions are U33, U11, U20 and U17, whereas U19 is affected by much larger deviations not only at the top but also at other locations. In this case, the (high) score can be used for deciding whether the computational approach used (code, model, mesh, etc.) could be successfully

Table A1

ranking by comparison with specific “target variables”.

MS_1 ($y = 7478 \text{ mm}$)			MS_19 (vent)			max(MS_1–MS_19)		
Ranking	User	Avg. Deviation	Ranking	User	Avg. Deviation	Ranking	User	Max avg. deviation
1	33	0.01052	1	17	0.006187	1	20	0.015122
2	20	0.015122	2	8	0.006326	2	33	0.017077
3	11	0.02112	3	33	0.00686	3	11	0.02112
4	39	0.02172	4	20	0.007129	4	17	0.0272
5	17	0.0272	5	11	0.007898	5	39	0.038856
6	8	0.0394	6	47	0.008551	6	8	0.039400
7	47	0.04084	7	32	0.008863	7	12	0.046345
8	12	0.046345	8	19	0.009593	8	47	0.049577
9	32	0.046512	9	42	0.010524	9	32	0.051511
10	19	0.05172	10	45	0.018294	10	19	0.054846
11	42	0.0532	11	41	0.021850	11	42	0.071923
12	37	0.057257	12	34	0.024031	12	41	0.09268
13	6	0.05896	13	12	0.026462	13	34	0.121320
14	34	0.0654	14	39	0.038856	14	45	0.121308
15	41	0.09268	15	37	0.057752	15	6	0.133374
16	45	0.09936	16	6	0.133374	16	37	0.208749

used for analyzing transients controlled by the same phenomena as those prevailing in this experiment.

Table A1 shows, however, that submission U8 is rather successful in predicting the erosion process, and very successful in predicting the mixing (very low score for the vent position, and maximum value coincident with that at the top). In reality, the inadequacy of the simulation to reproduce the main aspect of the transient is not revealed by the automatic processing of the errors. In fact, the helium concentration time-history at the top elevation along the injection axis (Fig. A1) shows that submission U8 is not able to predict the drop to the full mixing (equilibrium) value within the time of the simulation. The low average deviation (4%) is due to the fact that the experiment was terminated shortly after the mixing process was completed at the top of the vessel, and only few (four) measurement points were collected during the time after the mixing at the elevation of MS_1 (position B_18) occurred, which is the time where the actual difficulty of the simulation shows. Only these points (and the four before) render the actual measure of the discrepancy, but they are “diluted” in an average that includes the entire transient.

This example shows that the use of time averages for obtaining a measure of the accuracy of a simulation is questionable, at least for validation studies using experiments where large variations of the local variables occur during a short portion of the transient. On the other hand, also the use of the maximum deviation would fail to indicate that, for instance, U11 is able to predict the main phenomenon of interest (although the maximum deviation is about 13% like for U8) and U8 is not.

These considerations open the question of how to define a meaningful measure of the accuracy of a simulation when an automatic procedure to process the results is desired, without detailed inspection of the results and, first of all, of the data set used for the validation.

The question that follows from the previous one is whether any “score” or performance indicator can actually help in deciding whether the validation using a certain data set can be used for estimating the capabilities of a certain computational approach, and therefore if this qualifies for further investigations in more complex code assessment studies and could be eventually be taken into consideration for plant safety analysis.

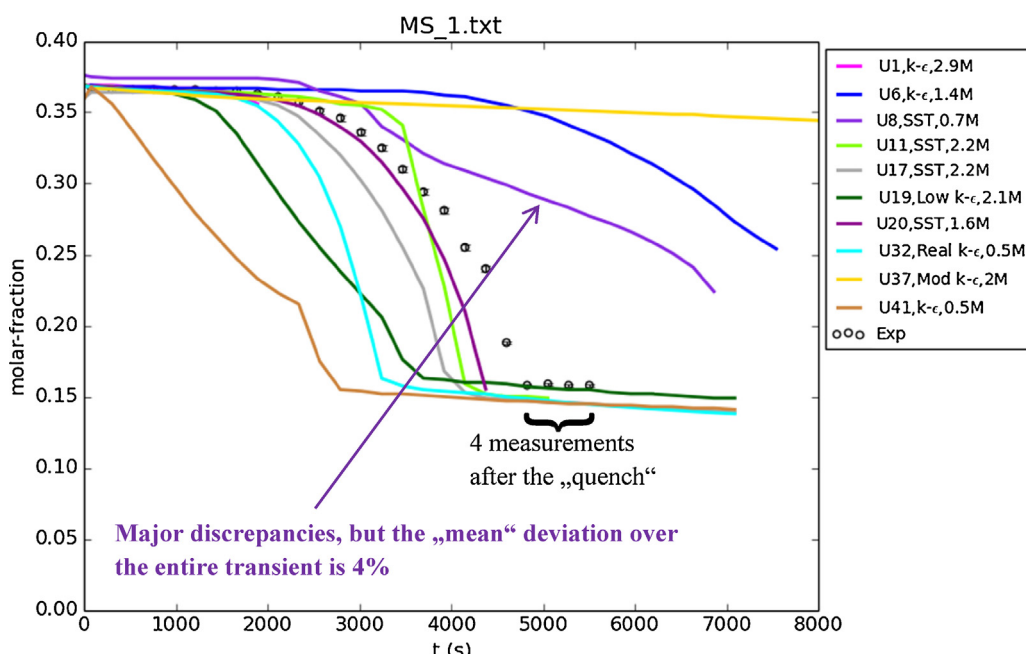


Fig. A1. Helium concentration at the uppermost measurement location along the injection axis.

It is recommended here that the first question will be addressed in future benchmark exercises, and that the second question will be well present in all considerations regarding the final purpose of this and connected activities.

References

- Allelein, H.-J., Fischer, K., Vendel, J., Malet, J., Studer, E., Schwarz, S., Houkema, M., Paillère, H., Bentaib, A., 2007. International standard problem ISP-47 on containment thermal hydraulics. In: Final Report NEA/CSNI/R(2007)10. Nuclear Energy Agency, Committee on the Safety of Nuclear Installations, pp. 2007.
- Andreani, M., Badillo, A., Kapulla, R., 2014. Synthesis of the OECD/NEA-PSI CFD benchmark exercise. In: Keynote Talk (KN01) Presented at the OECD/NEA Workshop on CFD Code Application to Nuclear Reactor Safety (CFD4NRS-5), 9–11 September, 2014, ETHZ, Zurich Switzerland.
- Andreani, M., Kapulla, R., Zboray, R., 2012. Gas stratification break-up by a vertical jet: simulations using the GOTHIC code. *Nucl. Eng. Des.* 249, 71–81.
- Boguslawski, L., Popiel, C.Z.O., 1979. Flow structure of the free round turbulent jet in the initial region. *J. Fluid Mech.* 90 (part 3), 531–539.
- Deri, E., Cariteau, B., Abdo, D., 2010. Air fountains in the erosion of gaseous stratifications. *Int. J. Heat Fluid Flow* 31 (5), 935–941.
- Kapulla, R., Mignot, G., Paladino, D., 2013. Dynamics of helium stratifications eroded by vertical air jets with different momenta. In: Proc. 15th International Topical Meeting on Nuclear Reactor Thermal Hydraulics (NURETH-15), Paper 192, 12–17 May, 2013, Pisa, Italy.
- Kapulla, R., Mignot, G., Paranjape, S., Paladino, D., 2014a. Stably stratified helium layer erosion by a vertical buoyant helium-air jet. In: OECD/NEA Workshop on CFD code Application to Nuclear Reactor Safety (CFD4NRS-5), 9–11 September, 2014, ETHZ, Zurich, Switzerland.
- Kapulla, R., Mignot, G., Paranjape, S., Ryan, L., Paladino, D., 2014b. Large scale gas stratification erosion by a vertical helium-air jet. *Sci. Technol. Nucl. Install.*, <http://dx.doi.org/10.1155/2014/197267>, Article ID 197267, 16 pages.
- Kelm, S., Ritterath, M., Prasser, H.-M., Allelein, H.-J., 2014. Application of the MINI-PANDA test case 'erosion of a stratified layer by a vertical jet' for CFD validation. In: OECD/NEA Workshop on CFD Code Application to Nuclear Reactor Safety (CFD4NRS-5), 9–11 September, 2014, ETHZ, Zurich, Switzerland.
- Lee, J.R., Kim, J., Song, C.-H., 2012. Synthesis of the OECD/NEA-KAERI rod bundle CFD benchmark exercise. In: CFD4NRS-4, 10–12 September, 2012, Daejeon, Korea.
- Lübbesmeyer, D., Aksan, S.N., May 2003. ISP42 (PANDA Tests) – Blind Phase Comparison Report. NEA/CSNI/R(2003)6.
- Mahaffy, J.H., 2010. Synthesis of results for the tee-junction benchmark. In: CFD4NRS-3, 14–16 September, 2010, Washington, DC, USA.
- Mi, J., Nobes, D.S., Nathan, G.J., 2001. Influence of jet exit conditions on the passive scalar field of an axisymmetric free jet. *J. Fluid Mech.* 432, 91–125.
- OECD-NEA-PSI CFD, 2013. OECD-NEA-PSI CFD Benchmark Specification. OECD-NEA-PSI CFD.
- OECD/NEA THAI Project, 22 June 2010. Hydrogen and fission product issues relevant for containment safety assessment under severe accident conditions. In: Final Report, Report NEA/CSNI/R(2010)3. OECD/NEA THAI.
- Paladino, D., Mignot, G., Kapulla, R., Zboray, R., Andreani, M., Tkatschenko, I., Studer, E., Brinster, J., 2013. OECD/SETH-2 project: PANDA and MISTRA experiments addressing key safety issues for water reactor containment. In: Proceedings of the 15th International Topical Meeting on Nuclear Reactor Thermalhydraulics (NURETH-15), Paper 106, 12–17 May 2013, Pisa, Italy.
- Rajaratnam, N., 1976. Turbulent Jets. Elsevier Scientific Publishing Company, New York, NY.
- Schwarz, S., Fischer, K., Bentaib, A., Burkhardt, J., Lee, J.-J., Duspiva, J., Visser, D., Kyttala, J., Royl, P., Kim, J., Kostka, P., Liang, R., 2011. Benchmark on hydrogen distribution in a containment based on the OECD-NEA THAI HM-2 Experiment. *Nucl. Technol.* 175 (3), 594–603.
- Smith, B.L., 2009. Identification and prioritization of generic nuclear safety problems requiring CFD analysis. In: Proc. 17th Int. Conf. on Nuclear Engineering (ICONE-17), Paper 75482, July 12–16, 2009, Brussels, Belgium.
- Smith, B.L., Mahaffy, J.H., Angele, K., Westin, J., 2011. Report of the OECD/NEA-Vattenfall T-Junction Benchmark Exercise. In: Report NEA/CSNI/R(2011)5.
- Smith, B.L., Song, C.-H., Chang, S.-K., Lee, J.R., Kim, J.W., 2013. Report of the OECD/NEA-KAERI rod bundle CFD benchmark exercise. In: Report NEA/CSNI/R(2013)5.
- Studer, E., Brinster, J., Tkatschenko, I., Mignot, G., Paladino, D., Andreani, M., 2012. Interaction of a light gas stratified layer with an air jet coming from below: large scale experiments and scaling issues. *Nuclear Eng. Des.* 253, 406–412.